UNIVERSITY OF HELSINKI

University of Helsinki
Dissertationes Universitatis Helsingiensis 248/2024

Using remote sensing to detect spatial patterns and phenology of peatland vegetation

Yuwen Pang

ACADEMIC DISSERTATION

Doctoral thesis, to be presented for public examination with the permission of the Faculty of Biological and Environmental Sciences of the University of Helsinki, in Biokeskus 2 Sali 2041, on 11th of October 2024, at 13 o'clock.

Author Yuwen Pang
Faculty of Biological and Environmental Sciences
University of Helsinki, Finland

Supervisors Docent Tarmo Virtanen
Faculty of Biological and Environmental Sciences,
University of Helsinki, Finland
Associate Professor Aleksi Räsänen
Geography Research Unit, University of Oulu, Finland
Docent Minna Väliranta
Faculty of Biological and Environmental Sciences,
University of Helsinki, Finland

Pre-examiners Senior Researcher Juan Pablo Arroyo Mora
National Research Council Canada, Canada
Senior Lecturer Angela Harris
University of Manchester, United Kingdom

Opponent Research professor Petteri Vihervaara
Finnish Environment Institute (Syke)

Custos Professor Atte Korhola
Faculty of Biological and Environmental Sciences,
University of Helsinki, Finland

Publisher: Helsingin yliopisto
Series: Dissertationes Universitatis Helsingiensis 248/2024

ISBN 978-952-84-0233-6 (print)
ISBN 978-952-84-0232-9 (online)
ISSN 2954-2898 (print)
ISSN 2954-2952 (online)
PunaMusta, Joensuu 2024

Abstract

The spatial and phenological patterns of peatland vegetation are closely linked to ecosystem functions, and can impact processes such as carbon sequestration, nutrient cycling, as well as biodiversity. It is essential to characterise these patterns to understand peatland ecosystems and their functioning. In addition, this knowledge can facilitate peatland management. Remote sensing (RS) technology offers extensive spatial coverage and frequent temporal observations, providing strong and broad application prospects in the spatio-temporal monitoring of ecosystems. Although the selection of specific RS data for various purposes has been studied, further investigation is needed to determine which technologies are most effective for peatland monitoring, such as whether multi-temporal and hyperspectral RS is required to accurately detect peatland vegetation conditions and dynamics.

This thesis consists of three case studies that investigated the utilisation of different RS data, including field spectroscopy, uncrewed aerial vehicle (UAV) hyperspectral (HS) and multispectral (MS) imagery, as well as Sentinel-2 (S2) satellite data to detect the spatial patterns and phenology of peatland vegetation in three northern peatlands. The objectives were 1) to recognise the advantages of multi-temporal RS data in detecting peatland vegetation characteristics (Papers I and III), 2) to determine whether HS features aid in mapping peatland vegetation (Papers I and II), and 3) to reveal the detectability of peatland vegetation patterns and its spatio-temporal dynamics (Papers I–III).

Field vegetation inventories were conducted in the studied peatlands, and the vegetation data were divided into three groups: community types obtained through ordination and fuzzy clustering methods, plant functional types, and individual plant species. Three vegetation characteristics—vegetation % cover, AGB, and LAI—were estimated and analysed across different vegetation groups. The random forest (RF) algorithm and its extensions were employed to build regression models and generate vegetation maps.

The field spectroscopy results indicated that multi-temporal RS data generally outperformed single-period models in predicting various peatland vegetation characteristics. Although no single-period model performed consistently well, the period of peak vegetation growth (mid-July to August) emerged as a viable alternative for achieving the best performance for most vegetation characteristics. Surprisingly, UAV HS did not facilitate vegetation mapping as expected, but it proved beneficial for certain plant functional types (PFTs) and plant species, whereas the UAV MS models exhibited relatively good performance in most cases. In the field spectroscopy analysis, spectral resolutions ranging from 1 nm to 20 nm produced the best models for predicting various vegetation characteristics. Furthermore, the seasonal development of AGB and LAI was delineated with field data and S2 datasets, revealing a unimodal seasonality that varied among plant communities and across landscapes. Overall, the three case studies suggested that the detectability of vegetation characteristics varied, and detectability to some extent varied between different peatlands. As expected, RS detection was more feasible at community and PFT levels than at the plant species level.

In summary, I emphasise the advantages of multi-temporal field spectroscopy while also recognising the potential utility of single-period data. I acknowledge the limited benefits of ultra-high spectral resolution and UAV HS compared to UAV MS data for mapping peatland vegetation. Additionally, time-series S2 datasets are valuable for tracking vegetation phenology in treeless peatlands. Notably, there is no one-size-fits-all RS strategy for peatlands, and the choice whether to use ultra-high spatial and spectral resolution data should be made based on the research objective. Therefore, I recommend careful consideration of the period and combination of RS data before initiating RS-based peatland research. By elucidating the utility of different RS datasets, I have provided valuable insights for monitoring vegetation patterns, which can inform future peatland management initiatives.

Acknowledgement

Finally, I have arrived at this moment and completed my PhD. Reflecting on this journey, I once thought I would have countless words to say, but now, as I stand here, I find myself at a loss. Instead, memories flood my mind. Let me take you back to January 9th, 2021, the day I first arrived in Finland. As I looked out of the plane window at the snow-covered landscape, I silently said to myself, "Wow, in this white and silent place, I will pursue my academic dreams and conduct the peatland research I love." Remarkably, after these years, I still hold onto that initial dream, and it has only grown stronger.

First and foremost, I would like to extend my heartfelt thanks to my Opponent, Petteri, my Custos, Atte, and my two Pre-examiners, Angela and Juan Pablo, who played a crucial role during the final stages of my PhD journey. I also wish to thank my thesis committee members, Anna and Markku, who followed my progress and provided valuable suggestions throughout my PhD journey.

I am deeply grateful to my three supervisors: Tarmo, Aleksi, and Minna. Because of you—because you stood by me and supported me—I was fearless and able to fully concentrate on my research. Tarmo and Aleksi, your rigor and vast knowledge in the research field have been invaluable. You taught me how to conduct research, from initiating research ideas, designing plans, testing methods, to writing manuscripts, all of which required countless hours of your review and comments. I could vividly recall my first fieldwork campaign, where I met wonderful colleagues from the University of Eastern Finland. I experienced many firsts: sleeping in tents, walking and working in the tundra, and enduring the mosquito season in Enontekiö and Inari. Though it was quite annoying at the time with thousands of mosquitoes swarming around me, it is now a beautified memory. A special thanks to Minna, the first person I reached out to, marking the true beginning of my PhD journey. You helped me with grant applications, coordination, and provided enduring support and warmth in my life.

I would like to thank all my co-authors and field collaborators—Franziska, Teemu, Tiina, Timo, Pasi, Mika, Viivi, and Milja—for their help during fieldwork and with manuscript writing and revisions. I could not have completed my PhD research as successfully without your support.

I have often said that I am incredibly lucky, and I believe I deserve this luck. I am delighted to have been part of the Climate Change Research Unit (ECRU), a harmonious group, we have spent several causal activities together, skinnies and bowling.

I have enjoyed sharing an office with my kind and friendly colleagues in Flexi Room 4619—Sanna P., Soila, Roxana, Tiia, Lilia, Ana, Sanna A., Emilia, Teemu and Salla—and spending coffee breaks with you in the coffee room. I have witnessed people come and go, celebrated your defences and graduations, and I am pleased to hear your subsequent successes.

Above all, I want to deeply thank my family! In Asian culture, it is difficult for me to express love directly, but we find ways to show it through actions, quiet support, and presence from a distance.

Over the years, I have learned to express my gratitude and love for them, cherish every moment, and allow our affection to flow more freely. I am so fortunate to be your daughter and your beloved youngest sister.

纸短情长，如何将我深深的爱述于纸上。不期于爱有来世，不假设你们知道：这一切一切都是为我而做，你们不说一句的爱有多深多好！茫茫人生好像荒野，家人是我永远能伏靠的肩膀，于是我将这所有的幸福和疼惜深深珍藏。在未来，我希望可以成为那个能让你们能依靠的女儿和妹妹！

Beyond my research, the most valuable lesson I have learned here is the importance of work-life balance. Outside the office, Kumpula Uniport became my second home, where I developed a love for dance and badminton—hobbies that I am certain will stay with me for life, along with my joy in being close to nature. The time I spent in group training classes and on the badminton court introduced me to many wonderful friends, who have brightened my days and uplifted my spirit.

I have shared unforgettable memories with friends: Zhang Mingzhen, Luo Danni, Ouyang Xiaodan, Zhao Siqi, Ying Huiyan, Chen Zhehao, Zhang ruoxi and Liu jianing. Our travels across many European countries are filled with tears and laughter, but if I had to pick a favourite, Iceland stands out! I have also enjoyed great weekends exploring the city and forests, as well as sharing meals with friends Cheng Ruoyu and Zhang Pei, many of which were organized by Guo Ming. Many old friends have come into my life and accompanied me along the way. There are so many of you who have helped and shared happy moments with me. Forgive me for not mentioning everyone by name, but I have packed all the memories with you in my heart!

Lastly, there is a Chinese saying that describes the moment when we first meet and grow closer, though every gathering eventually ends (相见时难别亦难，而天下无不散之宴席). I sincerely wish my dear supervisors, colleagues, and friends all the best. I will cherish my family. No matter what the future holds, these memories will empower me to overcome any challenges.

I sincerely wish all the best to my dear opponent, custos, pre-examiners, thesis committee members, supervisors, colleagues and friends. I wish my family happiness and health, and that we will always remain close. Whatever the future holds, these memories will give me the strength to overcome any challenges!

For the future, there is new beginning, and I will ‘With the power of knowledge – for the world!’.

庞毓雯 Yuwen Pang

At Viikii library, Helsinki, 4th of September, 2024

Table of Contents

Abstract III

Acknowledgement IV

List of original articles VII

List of abbreviations VIII

1 Introduction 1

1.1 Peatlands and their vegetation in global biogeochemical cycling 1

1.2 Remote sensing of peatland vegetation 3

1.3 Geographic object-based image analysis and statistical analyses 6

1.4 Objective of the study 7

2 Materials and Methods 9

2.1 Study sites 9

2.2 Vegetation data collection and processing 10

2.3 Remote sensing data collection and processing 12

2.4 Statistical analyses 14

3 Results 15

3.1 Multi-temporal RS data in peatland vegetation detection (Papers I and III) 15

3.2 Hyperspectral remote sensing for peatland vegetation detection (Papers I and II) 17

3.3 Spatio-temporal patterns of peatland AGB and LAI (Paper III) 23

4 Discussion 27

4.1 The benefits of multi-temporal RS data for detecting peatland vegetation (Papers I and III) 27

4.2 The role of HS features in peatland vegetation mapping (Papers I and II) 28

4.3 Detectability of spatial and temporal patterns of peatland vegetation characteristics (Papers I–III) 29

4.4 Limitations and future research 32

5 Conclusions 34

References 36

List of original articles

This thesis consists of three published research articles. These are referred by Roman numerals I-III in the text.

I. **Yuwen Pang**, Aleksi Räsänen, Viivi Lindholm, Mika Aurela and Tarmo Virtanen. (2022). Detecting peatland vegetation patterns with multi-temporal field spectroscopy, GIScience & Remote Sensing, 59:1, 2111-2126. DOI: 10.1080/15481603.2022.2152303

II. **Yuwen Pang**, Aleksi Räsänen, Franziska Wolff, Teemu Tahvanainen, Milja Männikkö, Mika Aurela, Pasi Korpelainen, Timo Kumpula and Tarmo Virtanen. (2024). Comparing multispectral and hyperspectral UAV data for detecting peatland vegetation patterns. International Journal of Applied Earth Observation and Geoinformation, 132, 104043. DOI: 10.1016/j.jag.2024.104043

III. **Yuwen Pang**, Aleksi Räsänen, Teemu Juselius-Rajamäki, Mika Aurela, Sari Juutinen, Minna Väliranta and Tarmo Virtanen. (2023). Upscaling field-measured seasonal ground vegetation patterns with Sentinel-2 images in boreal ecosystems, International Journal of Remote Sensing, 44:14, 4239-4261. DOI: 10.1080/01431161.2023.2234093

Authors' contributions

I. YP, AR, and TV developed the ideas of this study. AR and TV designed the fieldwork, VL collected field data, MA supported fieldwork, YP analysed the data and wrote the manuscript, AR and TV supervised the data analyses, and all authors commented and participated in writing.

II. YP, AR, and TV developed the ideas of this study. YP, TK, TT, TV and MM collected vegetation data, YP analysed the data and wrote the manuscript, AR and TV supervised the data analyses, and all authors commented and participated in writing.

III. YP, AR, and TV developed the ideas of this study. AR, TV and field assistants collected vegetation data; AR, YP, TJ, and TV processed the vegetation data; MA supported fieldwork and provided meteorological data; PK flighted the uncrewed aerial vehicle (UAV) and pre-processed UAV images; YP analysed the remote sensing data and wrote the manuscript; AR and TV supervised the data analyses; all authors commented and participated in writing.

List of abbreviations

%	Percentage
2D	Two-dimensional
3D	Three-dimensional
AGB	Aboveground biomass
DTM	Digital terrain models
FCM	Fuzzy c-means
FKM	Fuzzy k-medoids
GEOBIA	Geographic object-based image analysis
GHG	Greenhouse gas
HANTS	Harmonic analysis of time series
HS	Hyperspectral
LAI	Leaf area index
LiDAR	Light detection and ranging
MAE	Mean absolute error
MRF	Multivariate random forest
MRS	Multi-resolution segmentation
MS	Multispectral
nRMSE	Normalized RMSE
PFT	Plant functional type
QRF	Quantile regression forest
RF	Random forest
RMSE	Root mean square error
RS	Remote sensing
S2	Sentinel-2
S2A	Sentinel-2 A
SAR	Synthetic aperture radar
TP	Topographic or topography
UAV	Uncrewed aerial vehicle
SAR	Synthetic aperture radar
InSAR	interferometric SAR

1 Introduction

1.1 Peatlands and their vegetation in global biogeochemical cycling

Peatlands are among the largest carbon sinks in the biosphere; recent estimates suggest that northern peatlands alone store 500 ± 100 gigatons of carbon (Yu, 2012, Hugelius et al., 2020). In addition, peatlands provide other valuable ecosystem services, such as storing more than 10% of global freshwater, regulating the water cycle, reducing the risk of flooding, and protecting biodiversity by providing habitats for plants and wildlife (Kimmel and Mander, 2010). The cool and moist climate, along with the acidic and nutrient-poor soils in peatlands slow the decomposition rate of organic matter, which promotes peat accumulation over time and affects plant productivity (Rydin and Jeglum, 2013). In general, peatlands can function as both carbon sinks and sources (Leifeld et al., 2019), depending on various factors such as vegetation, hydrology, ground surface topography development, and other environmental conditions (Turetsky et al., 2014). Among these factors, peatland vegetation plays a crucial role in biogeochemical cycling via photosynthesis and respiration. For instance, it has been used as a proxy to estimate greenhouse gas (GHG) emissions (Couwenberg et al., 2011) and ecosystem production (Peichl et al., 2018).

Furthermore, peatland plant communities are distributed in response to hydrological and trophic conditions, shifting the ground surface to various microforms (Andersen et al., 2011). Typically, these microforms—hummocks/strings, lawns, and hollows/flarks—are visually distinct and identifiable, owing to their varying water table depths and representative plant compositions (Malhotra et al., 2016). Hummocks/strings are usually approximately a few centimetres to a meter above the ground surface and elevated above the water table, whereas hollows/flarks are usually situated below the water table level. Lawns, on the other hand, are located between hummocks and hollows, with a water table near the ground. Moreover, isolated microforms can blend into each other to form landscape mosaics, such as narrow string–wet flark–flat lawn landscapes, shaping spatial vegetation patterns (Rydin et al., 2006).

In addition to microforms, individual plant species and plant functional types (PFTs) display spatial patterns. There is several different PFT classifications, but northern

peatland researchers have commonly recognised seven PFTs in peatlands: deciduous shrubs, evergreen shrubs, forbs, graminoids, wet brown mosses, feather mosses, and *Sphagnum* (Laine et al., 2012, Rupp et al., 2019, Turetsky et al., 2012). Evergreen and deciduous shrubs (ericaceous shrubs in particular), along with small-leaved *Sphagnum* species such as *S. fuscum* and *S. capillifolium* are commonly found in hummocks and strings. In intermediate lawns, graminoids (e.g., *Cyperaceae* sedges), shrubs, forbs, and large-leaved *Sphagnum* species (e.g., *S. medium*) dominate, while water-loving graminoid species, forbs, and wet brown mosses are prevalent in hollows and flarks (Rydin and Jeglum, 2013).

On the other hand, vegetation phenology mainly reflects dynamic changes in plant greenness, such as leaf emergence and senescence, and is related to ecosystem processes throughout the seasons (e.g., (Koebsch et al., 2020, Kross et al., 2014)). In northern peatlands, snow cover lasts for a long period of the year, resulting in a unique seasonality of vegetation compared to other ecosystems (Zhao et al., 2015). During the spring thaw when the daily temperature rises above freezing, the ground vegetation begins to grow. Following such thaw and snow-free periods, bryophytes and evergreen shrubs become visible. Within a few weeks thereafter, the landscape turns green with leaves of deciduous shrubs and graminoids. In summer, leaf area grows rapidly, whereas in autumn, plants undergo senescence, and deciduous species lose their greenness and drop their leaves as solar radiation levels and daylight decrease. In addition, hydrological conditions are changing during the growing season, which impact to spectral properties of the peatland, and so also to vegetation pattern identification.

Due to the various physiological processes of different plant species, vegetation phenology varies among plant communities and PFTs, further characterising the seasonality of peatland biogeochemical cycles (Korrensalo et al., 2020, Leppälä et al., 2008). For instance, studies have shown that the phenology of plant communities drives seasonal trajectories of peatland ecosystem production (Peichl et al., 2018, Davidson et al., 2021). Deciduous and evergreen shrubs have been reported to have higher relative photosynthetic efficiencies than other vascular PFTs because of their long-lived woody shoots (Leppälä et al., 2008). Graminoids tend to mineralise their organic matter more quickly and have been found to have faster GHG exchange rates than shrubs and mosses (Dieleman et al., 2017). Mosses lack a vascular root system

and obtain nutrients from rainfall, forming symbiotic relationships with vascular plants and other organisms (Turetsky et al., 2012).

1.2 Remote sensing of peatland vegetation

Remote sensing (RS) is the science of observing and recording information about objects from a distance without direct contact (NASA, 2024). This is typically achieved using satellites (spaceborne), airborne platforms such as airplanes and uncrewed aerial vehicles (UAVs), as well as ground-based sensors (Table 1). RS sensors can be categorized based on their spectral resolution, which refers to their ability to distinguish between different wavelengths or spectral bands within the electromagnetic spectrum. A higher spectral resolution indicates a narrower spectral width, allowing the sensor to detect a greater number of narrow spectral bands. Generally, RS sensors fall into two categories based on spectral resolution: multispectral (MS), which typically contains up to a dozen spectral bands, and hyperspectral (HS), which contains tens to hundreds of spectral bands. In the context of peatlands, RS data have been extensively utilized over the years, with UAVs gaining popularity due to advances in portable MS and HS sensors (Czapiewski and Szuminska, 2022, Abdelmajeed and Juszczak, 2024).

Table 1 List of main characteristics of some high-resolution optical remote sensing data for peatland vegetation research

Platform	Sensor: multi- or hyper- spectral	Spectral range or/and No. of bands	Spatial resolution [m]	Temporal resolution [day]
Sentinel-2 (satellite)	MSI: multi	13 bands	10–60	5
PlanetScope (satellite)	PlanetScope Camera: multi	450–800 nm, 8 bands	3	Able to a daily collection
Worldview 2 &3 (satellite)	WorldView-110 camera: multi	450–800 nm, 8 bands	1.2–1.8	Up to 1.1
QuickBird (satellite)	Ball Global Imagery System 2000: multi	450–900 nm, 4 bands	2.4–2.6	2.5 or less
	SPECIM AFX10: hyper	112 or 224 bands	0.07 (at 100 m altitude)	
UAVs (airborne, DJI drone etc.)	Senop Rikola: hyper	500–900 nm, 28 bands	0.65 (at 100 m altitude)	Up to orders or demands
	Micasense rededge-M: multi	5 bands	0.77 (at 120 m altitude)	

	Onboard camera: multi	3 bands: RGB	0.02 (at 100 m altitude)
Spectroradiometers (in-situ)	ASD FieldSpec pro: hyper	350–2500 nm	Depends on the set-up height
	ASD FieldSpec 3/4: hyper	350–2500 nm	Depends on the set-up height

Different RS datasets have their own advantages in conducting various vegetation studies, but comparative studies of their specific uses and capabilities have not been fully conducted in peatlands thus far (Abdelmajeed and Juszczak, 2024). Field spectroscopy collected by spectroradiometers with hundreds of spectral bands has been successfully utilised in various applications, such as the classification of plant communities (Erudel et al., 2017), PFTs (Kattenborn et al., 2019, Rebelo et al., 2018), and plant species (Bubier et al., 1997), as well as the derivation of vegetation characteristics, such as % cover (Schaepman-Strub et al., 2009), AGB (Mohammedshum and Kooistra, 2015), and LAI (Onodi et al., 2017). However, it is limited to covering the area of a small plot (e.g., < 1 m^2), primarily restricting its utility in field investigations. UAV data have been used to address the trade-off between the coverage area and high-resolution data quality. UAVs equipped with MS or HS have been successfully applied to delineate vegetation spatial distributions (Steenvoorden et al., 2023, Räsänen and Virtanen, 2019, Bertacchi et al., 2019) and predict vegetation AGB and LAI (Räsänen et al., 2020, Assiri et al., 2023). In addition, satellite data show great potential for various landscape-level missions because of their regular revisits and coverage of regional scales. For instance, the Sentinel-2 (S2) constellation's A and B satellites have a 5-day revisit cycle, making them particularly useful for vegetation phenology purposes (Misra et al., 2020). As such, they have been used for tracing the seasonal development of vegetation AGB and LAI (Juutinen et al., 2017, Garisoain et al., 2023, Linkosalmi et al., 2022).

RS data can be acquired during a single period or across multiple periods of time. It is necessary to clarify the role of collection period and data combination in RS-based studies in which several examinations have been conducted. For instance, Cole et al. (2014a) and Beamish et al. (2017) identified specific periods of RS data collection that differentiate target plant communities, whereas others argue that multi-temporal data are more likely to enhance the classification of peatland vegetation (Dudley et

al., 2015, Erudel et al., 2017). However, research comparing how single- and multi-temporal data affect the detection of spatial patterns in peatland vegetation is limited.

Furthermore, multi-temporal RS data are typically applied in phenological studies, but both in-situ spectrometers and UAVs have limitations in this regard. Field spectroscopy collection across seasons is labour-intensive and covers only the sample plot area. In contrast, UAV data can cover many hectares depending on the number of flights, but is generally more expensive, and costs increase significantly when frequent missions are required. To meet the requirements for revisiting and increasing spatial coverage, researchers have applied S2 data to produce landscape-level maps of vegetation AGB and LAI (e.g., (Räsänen et al., 2021, Fassnacht et al., 2021)). However, in phenological studies, the focus primarily revolves around linking vegetation dynamics to GHG exchanges (e.g., (Linkosalmi et al., 2022, Junttila et al., 2021)), with fewer studies examining vegetation characteristics directly with RS. For example, by using S2 datasets, Juutinen et al. (2017) derived vegetation LAI phenology in arctic tundra, Tian et al. (2021) compared vegetation greenness phenology across Europe, and Garisoain et al. (2023) explored *Sphagnum* LAI phenology in mountain peatlands. Overall, the potential of S2 data to track vegetation phenology across boreal ecosystems has not been fully tested, and it remains unclear whether S2 data at coarse spatial resolutions (10–60 m) are suitable for capturing vegetation phenology among peatland plant communities, because of the high spatial heterogeneity in these landscapes.

On the other hand, there is a trend in vegetation applications to integrate multi-source remote sensing data, such as combining HS, MS, and radar sensors. Because of the spectral diversity in spatially heterogeneous environments, HS RS has been shown to be statistically more effective than MS RS in wetlands (Adam et al., 2010). However, a review of the literature on this topic also highlighted that the contribution of HS data is complex, owing to the different characteristics and environments, suggesting the need to explore its additional role in detecting peatland vegetation (Dronova et al., 2021). HS datasets are also much larger and require more effort to collect and process than simpler MS datasets. Additionally, it has been reported that the UAV multi-source framework is beneficial for several vegetation detections, such as plant community classification (Beyer et al., 2019) and vegetation AGB and LAI estimation (Assiri et al., 2023). Moreover, attention has been paid to the value of

adding light detection and ranging (LiDAR) to UAV optical data to delineate the spatial patterns of vegetation (Korpela et al., 2020, Assiri et al., 2023). To the best of my knowledge, the contribution of HS data to facilitating peatland vegetation detection, such as their relative benefits in different RS data combinations, remains poorly known.

1.3 Geographic object-based image analysis and statistical analyses

In recent years, geographic object-based image analysis (GEOBIA) has emerged as a powerful tool for extracting information from RS data, particularly when utilized with ultra-high spatial resolution data containing detailed land surface information. This approach offers a more efficient and accurate method for analysing complex landscapes, like peatlands (Blaschke et al., 2014, Berhane et al., 2018). GEOBIA typically involves third steps: (1) image segmentation, (2) feature extraction, and (3) subsequent image analysis (Hossain and Chen, 2019). During segmentation, image pixels are grouped into polygonal objects based on the spectral, textural, geometric, and contextual features of the neighbouring pixels. Feature extraction refers to extracting meaningful RS features, such as spectral bands, spectral indices, shape and texture attributes from segmented objects. The constructed feature datasets are then used for subsequent processes, such as land cover classification and regressions (Kucharczyk et al., 2020).

GEOBIA offers several advantages over traditional pixel-based image-analysis methods. By performing a segmentation step, GEOBIA groups square image pixels into meaningful objects, providing a more comprehensive representation of features in the image and improving the accuracy of the feature extraction and subsequent analysis (Hossain and Chen, 2019). Additionally, GEOBIA allows for the semantic interpretation of objects, enabling a deeper understanding of complex spatial patterns and structures. Combining contextual information from neighbouring pixels can also reduce the effects of noise and spectral variability, which is particularly helpful in spectrally complex environments such as wetlands (Du et al., 2021, Berhane et al., 2018). Moreover, researchers have pointed out that the accuracy of feature extraction and analysis mainly depends on the quality of image segmentation (Su and Zhang, 2017). In this thesis, multi-resolution segmentation (MRS) (Baatz and

Schäpe, 2000) was adopted for its success in many RS application domains (Witharana and Civco, 2014).

Machine learning techniques such as the random forest (RF) algorithm and its extensions, including multivariate random forest (MRF) and quantile regression forest (QRF), are typically performed to construct regression models between response variables and RS predictors. RF aggregates the outputs of multiple decision trees to generate a single result, and is robust in handling non-normality and outliers (Breiman, 2001). It has demonstrated strong performance in both spatial and temporal modelling (Hengl et al., 2018) and has been shown to outperform other machine learning methods in wetland vegetation applications (Jafarzadeh et al., 2022). Regarding the other two extensions, MRF, known for its ability to handle multiple response variables simultaneously, is most effective when some response variables are correlated or related (Segal and Xiao, 2011). During the training process, MRF considers the relationships between the response variables to enhance the overall prediction accuracy compared with using separate RF models for each response variable. The QRF combines the principles of quantile regression with RF and is particularly valuable for estimating conditional quantiles, offering a more comprehensive understanding of the conditional distribution of the response variable (Meinshausen, 2006).

1.4 Objective of the study

In this thesis, I aimed to determine the spatial patterns and phenology of peatland vegetation characteristics, vegetation % cover, AGB, and LAI using different RS data. This thesis answers the following research questions (Figure 1):

1) Can multi-temporal RS data enhance the detection of various peatland vegetation characteristics compared with single-period RS data? (**Papers I and III**)

2) Do HS RS data facilitate peatland vegetation mapping that includes community types, PFTs, and plant species? (**Papers I and II**)

3) How detectable are peatland vegetation patterns, and what are its spatio-temporal patterns? (**Papers I–III**)

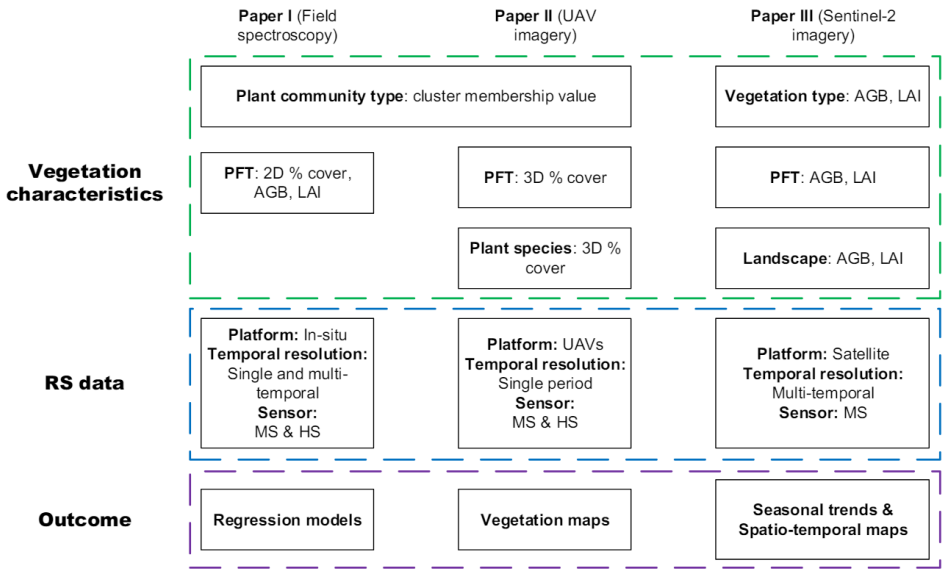


Figure 1 Outline of this thesis. UAV refers to uncrewed aerial vehicle, PFT refers to plant functional type, 2D/3D % cover refers to two-/three-dimensional % cover, AGB refers to aboveground biomass, LAI refers to leaf area index, and MS/HS refers to multispectral/hyperspectral.

2 Materials and Methods

Three northern peatlands were selected from Finnish Lapland. Five separate field vegetation inventories were conducted, and three types of RS data were collected: field spectroscopy, UAV MS and UAV HS imagery, and S2 imagery. Vegetation data were organised into community types using ordination, fuzzy c-means (FCM), and fuzzy k-medoids (FKM), and into PFTs. Moreover, the case studies focused on various vegetation characteristics, such as membership values for community types, vegetation % cover, AGB, and LAI for PFTs. The RS data were processed by spectral resampling, GEOBIA, and spectral index calculations. Finally, RF, MRF, and QRF were utilised to build regression models between the vegetation and RS variables in the case studies (Table 2).

Table 2 Summary of materials and methods

Paper	Study site	Vegetation data	Remote sensing data	Method
I	Lompolojänkkä Halssiaapa	Bi-weekly vegetation field inventories in 2019	Bi-weekly field spectroscopy	Fuzzy c-means (FCM) Multivariate random forest (MRF)
II	Halssiaapa	One-time vegetation inventory in 2022	Uncrewed aerial vehicle (UAV) multispectral (MS) and UAV hyperspectral (HS) imagery	Fuzzy k-medoids (FKM) Geographic object-based image analysis (GEOBIA) Random forest (RF)
	Kaamanen	One-time vegetation inventory in 2021		
III	Pallas Sodankylä (Halssiaapa)	Bi-weekly vegetation field inventories in 2019	Time-series Sentinel-2 (S2) datasets	FCM RF Quantile regression forest (QRF)
	Kaamanen	Bi-weekly vegetation field inventories in 2017		

2.1 Study sites

The study areas comprised three northern peatlands in Finnish Lapland (67°–69° N), presenting distinct biological, geological, climatological, and topographical characteristics (Figure 2). These sites have been studied by the Finnish Meteorological Institute for carbon dynamics and related topics (Maanavilja et al., 2011, Dinsmore et al., 2017, Aurela et al.,

2015), highlighting the continued interest in accurately mapping their vegetation. Moving from south to north in Sodankylä, the Halssiaapa fen (67°22' N, 26°39' E, 180 m a.s.l., **Papers I–III**) features a string–lawn–flark microtopography. In the Pallas region, the Lompolojänkkä fen (67°59' N, 24°12' E, 269 m a.s.l., **Papers I and III**) is characterised by its open, flat terrain and nutrient-rich environment, whereas the Kenttärova forest (67°59' N, 24°14' E, 347 m a.s.l., **Paper III**) is dominated by Norway spruce (*Picea abies*) with a mix of deciduous trees. In the northernmost part, the Kaamanen fen (69°8' N, 27°16' E, 155 m a.s.l., **Papers II and III**) displays apparent dry string and wet flark landscape mosaics. Over the period of 2008–2023, the mean annual air temperatures and mean total precipitation were as follows: 0.83 °C and 591 mm in Halssiaapa, 0.37 °C and 686 mm in Pallas, and 0.09 °C and 457 mm in Kaamanen, respectively.

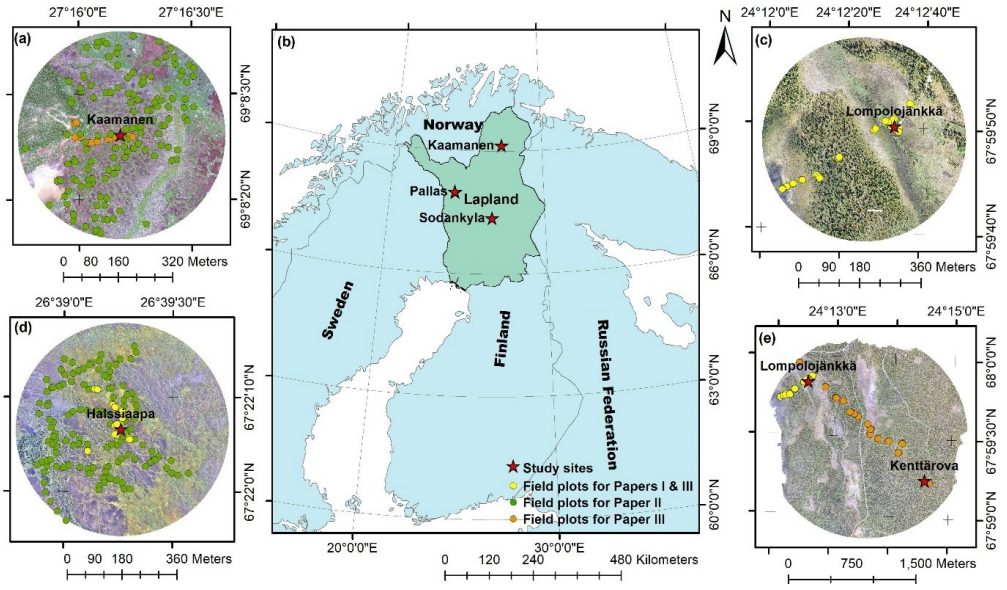


Figure 2 Locations of study sites and field plots (b), and (a) Kaamanen fen, (d) Halssiaapa fen in Sodankylä and (c) Lompolojänkkä fen and (e) Kenttärova forest in the Pallas region.

2.2 Vegetation data collection and processing

Five separate field vegetation inventories were conducted between 2017 and 2022. Although the sampling scheme remained consistent during each campaign, there were differences between campaigns in terms of the number and shape of plots (i.e., round or square) and sampling frequency (i.e., once or every two weeks) (Table 3).

Some characteristics are commonly used to capture vegetation spatial patterns and phenology, including vegetation percentage (%) cover, aboveground biomass (AGB), and leaf area index (LAI) (e.g., (Laine et al., 2012, Garisoain et al., 2023, Cole et al., 2014a)). Percentage cover refers to the proportion of the ground surface covered by vegetation. In its two-dimensional (2D) form, it corresponds to the above view (Räsänen et al., 2020, Juutinen et al., 2017), while in its three-dimensional (3D) form, it provides information regarding the vertical layering of vegetation. AGB represents the amount of organic matter stored in vegetation above the ground and is typically measured in units of mass per unit area (e.g., grams per square meter), thereby providing an estimate of the vegetation carbon stock (Verwijst and Telenius, 1999). LAI quantifies the amount of foliage present in a vegetation canopy per unit ground area and is usually expressed as a dimensionless ratio, serving as a surrogate for the photosynthetic capacity of vegetation (Chen and Black, 1992). These vegetation characteristics reflect biogeochemical cycles of ecosystems and are interrelated. For instance, % cover and vegetation height is commonly used to estimate AGB and LAI in non-destructive models (Goud et al., 2017).

The % cover of identified plant species (or genera) was estimated from the 2D (projected coverage, totalling 100%) and/or 3D (totalling$\geqslant$ 100%) perspectives. For shrubs, the 2D % cover was quantified separately for the green and brown (woody parts) proportions. The mean height of the vascular plants was measured using a ruler. The locations of all plots were measured by real-time kinematic positioning using a Trimble R10 GNSS device with an accuracy of 5 cm.

During data processing, field plots were assigned into plant communities based on plant species (or genera) 2D % cover using non-metric multidimensional scaling ordination and FCM or FKM clustering. Additionally, plant species (or genera) were grouped into seven PFTs: deciduous shrubs, evergreen shrubs, forbs, graminoids, wet brown mosses, feather mosses, and *Sphagnum*. Furthermore, vegetation AGB and LAI were estimated using the 3D % cover and heights at the PFT level via empirical regression-based equations.

Table 3 Summary of vegetation data (some abbreviations are first described in Table 1.)

Paper	Study site	Sampling period	Vegetation plot	Description	Vegetation characteristics

I	Lompolojänkkä	Bi-weekly revisit, between May and August, in 2019	39	Circular plots with a 50-cm diameter	FCM plant community clusters; Two dimensional (2D) % cover, above ground biomass (AGB) and leaf area index (LAI) of plant functional types (PFTs)
	Halssiaapa		43		
II	Kaamanen	One-time visit, in late July 2021	132	Square plots with a 50-cm side length	FKM plant community clusters; Three dimensional (3D) % covers of plant species and PFTs
	Halssiaapa	One-time visit, in late July 2022	135		
III	Pallas	Bi-weekly revisit, between May and August, in 2019	39 in Lompolojänkkä fen (reused from Paper I) 45 in Kenttärova forest	Circular plots with a 50-cm diameter	FCM plant community clusters; Landscape LAI and AGB
	Sodankylä (Halssiaapa)		43 (reused from Paper I)		
	Kaamanen	Bi-weekly revisit, between May and October, in 2017	18		

2.3 Remote sensing data collection and processing

Various RS data were used and processed in the case studies to address the specific research questions (Table 4). In **Paper I**, biweekly field spectroscopy was performed using an ASD Handheld II spectroradiometer (Analytical Spectral Devices, Boulder, CO, USA). The spectral data, covering wavelengths between 400 and 900 nm, underwent spectral normalisation and Savitzky–Golay filtering. Additionally, the pre-processed spectra at 1 nm spectral intervals were resampled to four other sampling intervals: 5, 10, 20, and 50 nm, and simulated for two types of band combinations of the Sentinel-2 A (S2A) satellite: S2A-4 (blue (B2), green (B3), red (B4), and near-infrared (B8)) and S2A-8 (S2A-4 bands, red edge (B5), and near-infrared (B6, B7, and B8A)).

In **Paper II**, 5-band UAV MS and 112-band UAV HS images were obtained through field flights, and LiDAR-based digital terrain models (DTMs) were collected from the

National Land Survey of Finland. The UAV images were first subjected to geometric and radiometric calibrations, then spectral indices were calculated, and LiDAR-DTMs were used to derive eight topographic features. For analysis, within the GEOBIA framework, the UAV MS imagery was segmented using MRS, and features from MS and HS datasets (bands and indices)— including TP features—were extracted for the segments to build four types of RS datasets: MS (multispectral features only), MS+TP (multispectral and topographic features), HS MS (hyperspectral features only), and HS+TP (hyperspectral and topographic features).

In **Paper III**, time-series Sentinel-2 Level-2A (S2 L2A, bottom of atmosphere reflectance) images were collected with a 10% cloud threshold, and spectral indices were calculated. To mitigate the effects of irregular S2 image acquisition dates, harmonic analysis of the time series (HANTS) was used to reconstruct the S2 dataset. Since the cloudless images in Kaamanen were insufficient, this site was excluded from the Sentinel-2-based analysis.

Table 4 Summary of remote sensing data and processing and analysis methods (abbreviations are firstly described in previous tables)

Paper	Study site	Remote sensing data	Processing method	Statistics analysis
I	Lompolojänkkä and Halssiaapa	Bi-weekly field spectroscopy during May and August in 2019	Conduct spectral noise filtering and spectral resampling	MRF and validation of the models by averaging over 20 runs
		UAV HS imagery (SPECIM AFX10), on 24 Jul 2022 in Halssiaapa / 29 Jul 2021 in Kaamanen	Calculate 79 HS indices	
II	Halssiaapa and Kaamanen	UAV MS imagery (Micasense RedEdge), on 24 Jul 2022 in Halssiaapa /29 Jul 2021 in Kaamanen	Calculate 7 MS indices and implement GEOBIA	RF and validation of the models by 10-fold cross-validation
		LiDAR-derived digital terrain models (DTMs)	Calculate 8 topographic (TP) features	
III	Pallas and Sodankylä (Halssiaapa)	Time series S2 datasets during May and September in 2019	Calculate spectral indices and implement harmonic analysis of time series (HANTS)	RF, and QRF for uncertainty analysis, and validation of the models by averaging over 20 runs

2.4 Statistical analyses

Different statistical methods were used in the case studies. In **Paper I**, the MRF algorithm was employed to construct regression models between field spectroscopy datasets and vegetation variables, including FCM membership values of plant community clusters, and 2D % cover, AGB, and LAI of PFTs. To examine the influence of time periods and spectral resolution on model performance, regressions were built using different field spectroscopy data from individual collection dates or over the whole season, as well as five spectral resampling intervals (1–50 nm) and two types of S2A band simulations: S2A-4 and S2A-8. In **Paper II**, the RF algorithm was used to build regression models between four types of UAV datasets: HS, HS+TP, MS, MS+TP, and FKM membership values of plant community clusters and 3D % cover of PFTs and plant species. Furthermore, feature importance was assessed using the Gini index. Therefore, the relative contributions of the HS features in the regressions were compared. In **Paper III**, RF regressions were built on time-series S2 datasets and field-measured vegetation AGB and LAI, respectively.

To validate the regression models in **Paper I**, the percentage of explained variance rate (also known as pseudo R^2), root mean square error (RMSE), and normalised RMSE (nRMSE) were calculated and averaged over 20 runs for each regression. In **Paper II**, the explained variance rate, mean absolute error (MAE), and RMSE were computed. In **Paper III**, in addition to calculating the average explained variance, RMSE, and nRMSE over 20 runs of all RF regressions, QFR was implemented on the RF regressions for uncertainty analysis, providing a symmetric 95% prediction interval with 0.025 lower and 0.975 upper quantiles.

3 Results

3.1 Multi-temporal RS data in peatland vegetation detection (Papers I and III)

Regression models based on multi-temporal field spectroscopy outperformed single-date models, with explained variances ranging from 43% to 48% for plant communities and from 43% to 70% for PFTs at the two study sites (Figure 3 and Figure 4, **Paper I**). On average, whole-season models improved the variance explained by single-date models by 14–25% for plant communities and 10–33% for PFTs.

However, a single period can still yield good modelling results, offering an alternative to whole season models, such as August, for hummock communities (Figure 3 and Figure 4, **Paper I**). Regarding PFTs, models based on single-date spectroscopy varied greatly, with some PFTs or vegetation categories showing notably poor predictions. Only a few periods performed well, such as August for evergreen shrubs and June and July for graminoids.

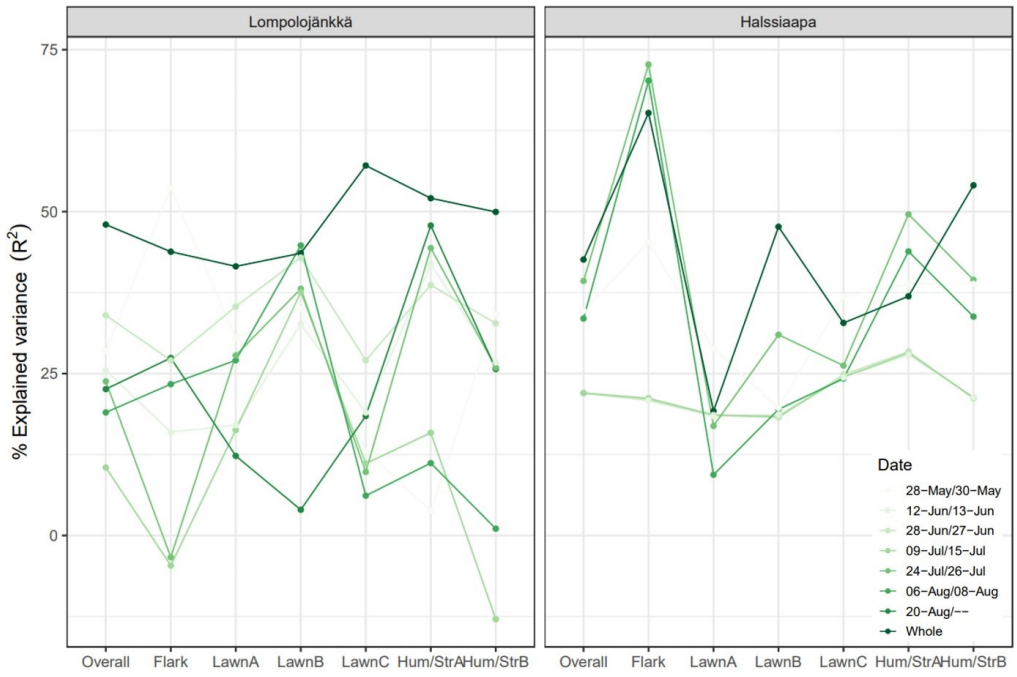


Figure 3 Performance of regression models for plant communities based on whole-season and single-date spectroscopy data. Hum/Str refers to hummock/string.

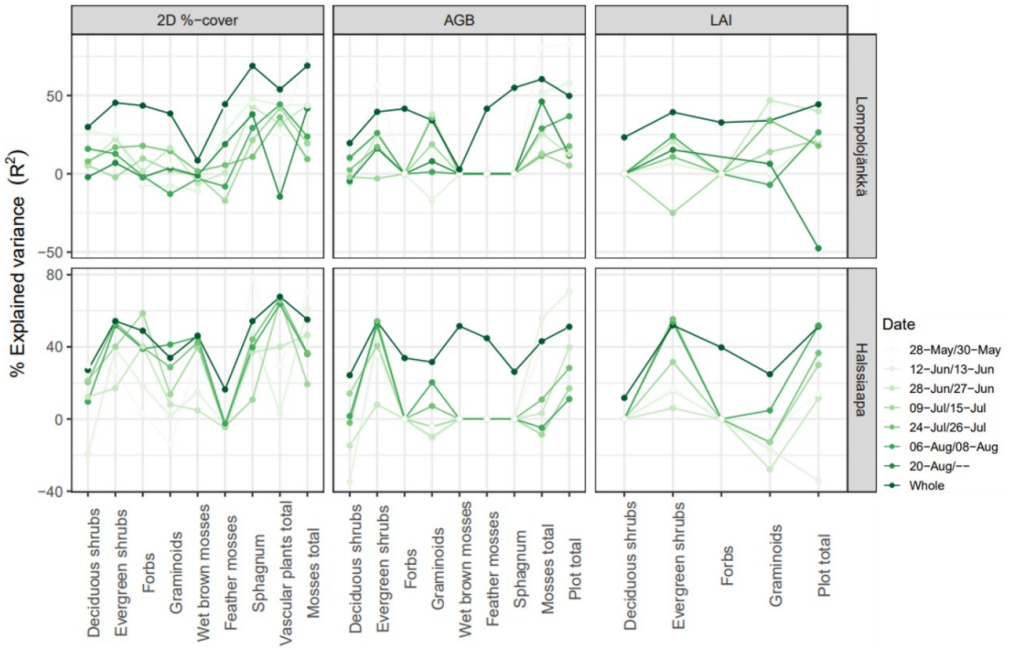


Figure 4 Performance of regression models for two-dimensional (2D) % cover, above ground biomass (AGB), and leaf area index (LAI) by plant functional type (PFT) and vegetation category, based on whole-season and single-date spectroscopy data.

On the other hand, the time-series S2 dataset-based regression models generated variance explained rates of 24–50% for predicting ground layer AGB and 49–56% for LAI at the two sites (Figure 5, **Paper III**). Sodankylä showed relatively better modelling for both AGB and LAI than Pallas, with higher R2 and lower RMSE values. Some vegetation types were poorly predicted. For instance, AGB appeared to be overestimated in sedge fens and flarks, whereas LAI was underestimated in the willow thickets. Moreover, extremely low and high AGB and LAI values were more likely to be misestimated by S2 models. For example, the S2 model overestimated the AGB < 250 g m-2 in field measurements, resulting in data points deviating from the 1:1 line.

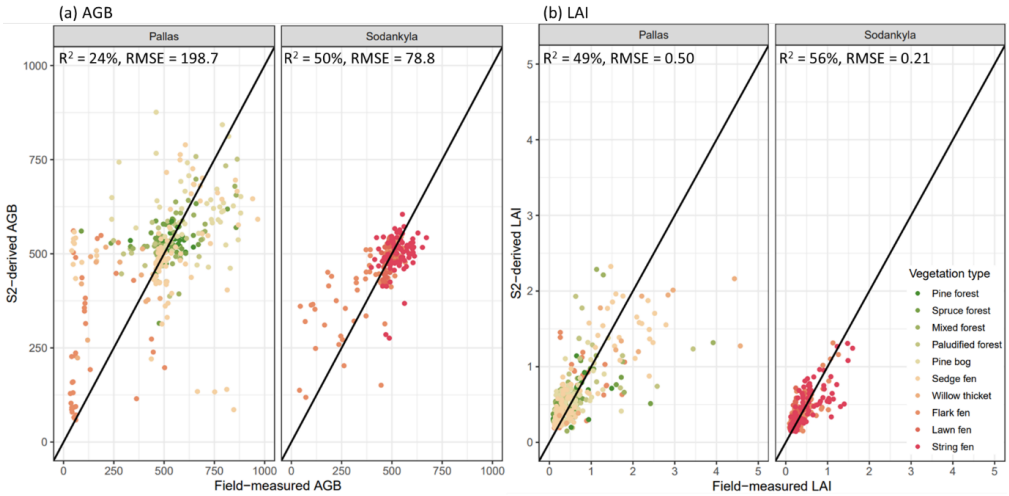


Figure 5 Scatter plots between field-measured and S2-derived (a) AGB (g m^{-2}) and (b) LAI annotated by vegetation community type. R^2 refers to the percentage of variance explained rate, RMSE refers to the root mean square error in the random forest regression models, and the solid lines refer to the 1:1 identity line.

3.2 Hyperspectral remote sensing for peatland vegetation detection (Papers I and II)

The detectability of plant communities and PFTs (including the three vegetation categories) varied greatly among the different spectral resolutions (Figure 6 and Figure 7, **Paper I**). Generally, the best modelling performance was observed with a spectral resolution of 1–20 nm, resulting in an explained variance of 43–48% for communities and 3–70% for PFTs.

For most plant communities, there was a downward trend in the variance explained at coarser spectral resolutions, although the narrowest spectral separation at 1 nm did not consistently ensure the best models (Figure 6, **Paper I**). Furthermore, the variance explained rates differed slightly between models based on 1 nm to 20 nm spectral resolution but were much lower for models on the 50 nm and S2A band simulations, declining by 5% and 7% from the best predictions, respectively. In contrast, for the PFTs and vegetation categories, S2A-8 still achieved relatively good predictions compared to the high spectral resolution models (i.e., 1–20 nm) (Figure 7, **Paper I**).

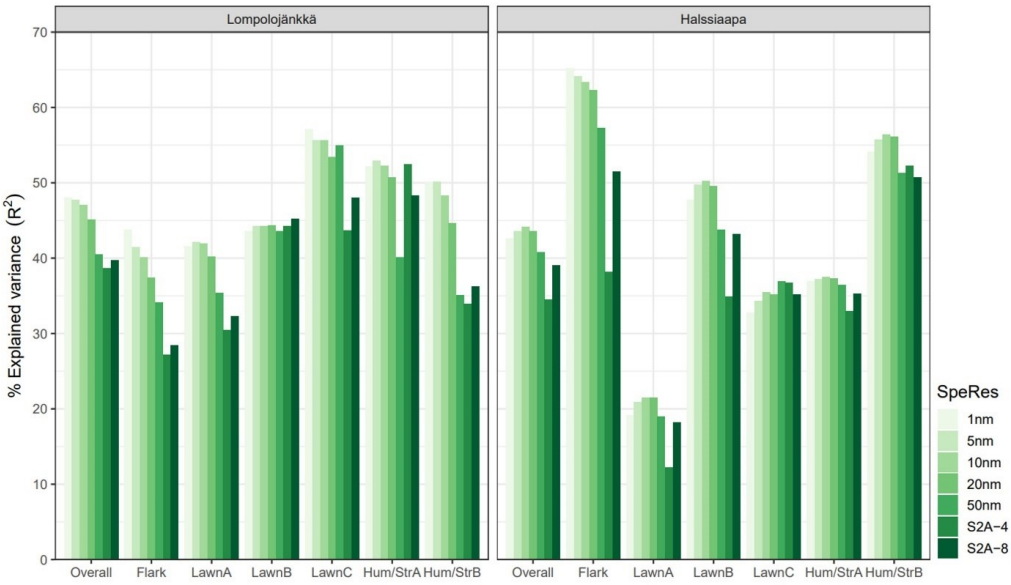


Figure 6 Performance of regression models for plant communities based on seven spectral resolution (SpeRes) groups. Hum/Str refers to hummock/string.

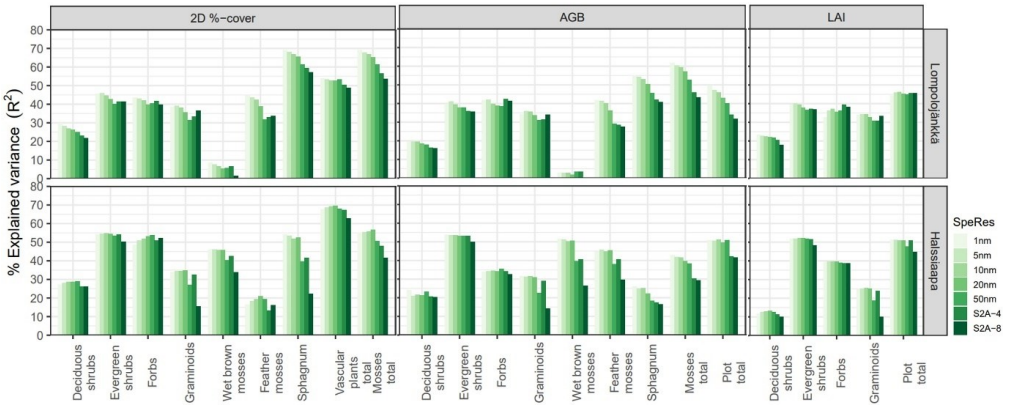


Figure 7 Performance of regression models for PFTs and vegetation categories based on seven spectral resolution (SpeRes) groups.

When comparing the four types of UAV data-based models (HS, HS+TP, MS, and MS+TP), none consistently outperformed the others in predicting all three vegetation categories, leading to varying explained variance rates (Figure 8, **Paper II**). Nevertheless, each model showed advantages; for example, the HS+TP setup excelled overall in Halssiaapa, whereas the MS models performed relatively well in Kaamanen. Plant community types generally yielded better modelling results than PFTs and plant species, with variance explained rates ranging from 44% to 56% for

plant community types, 32% to 55% for PFTs, and 30% to 46% for plant species across the two study sites.

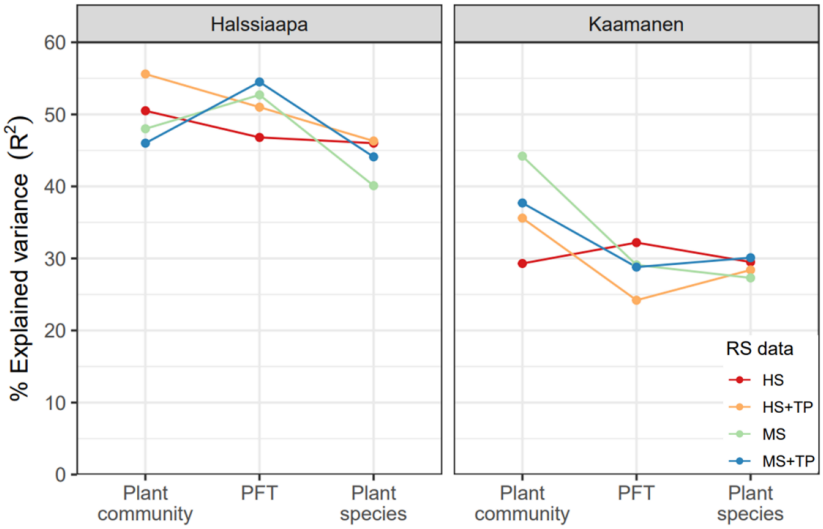


Figure 8 Performance of regression models for three vegetation categories using four types of RS datasets: UAV hyperspectral features only (HS), UAV hyperspectral and topographic features (HS+TP), UAV multispectral features only (MS), and UAV multispectral and topographic features (MS+TP).

Model performance varied widely for specific vegetation characteristics (Figure 9, **Paper II**). Furthermore, TP features may be advantageous in certain cases, whereas in others, they result in predictions that are comparable to—or even worse than—the spectral-only options.



Figure 9 Performance of regression models for individual vegetation characteristics of, (a) plant community, (b) PFT, and (c) plant species, using four types of RS datasets: HS, HS+TP, MS, and MS+TP.

Regarding the importance of features in the regression models, the HS spectral indices held the highest positions in the HS+TP models. However, for the MS+TP modelling option, certain MS spectral indices and bands were influential in Halssiaapa, whereas in Kaamanen, the significance of several TP features was notably higher (Figure 10, **Paper II**).

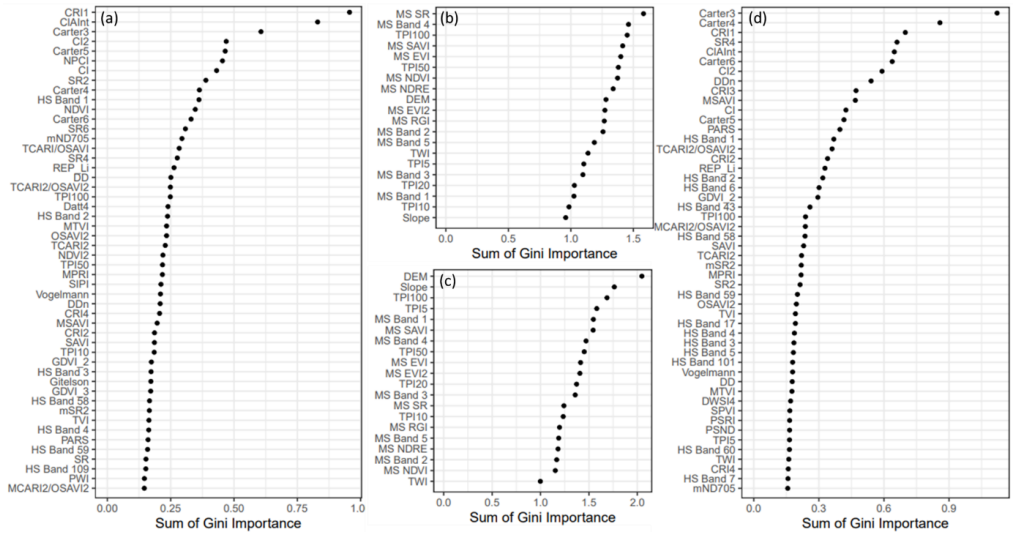


Figure 10 Feature importance rate: listing all features in MS+TP models and the top 50 important features in HS+TP models sorted using the Gini method. (a) and (b) represent the HS+TP and MS+TP models, respectively, in Halssiaapa, whereas (c) and (d) represent the HS+TP and MS+TP models, respectively, in Kaamanen.

Final vegetation maps were created based on the HS+TP and MS+TP models (Figure 11 and Figure 12, **Paper II**). The distribution of PFTs and plant species was correlated with the plant community clusters. For example, in Halssiaapa, *Sphagnum* dominated flarks, and *Andromeda polifolia* grew along the strings and in drier parts of the lawns, and in Kaamanen, graminoids were most common near stream and lawns, and *Carex limosa* was growing mainly in flarks.

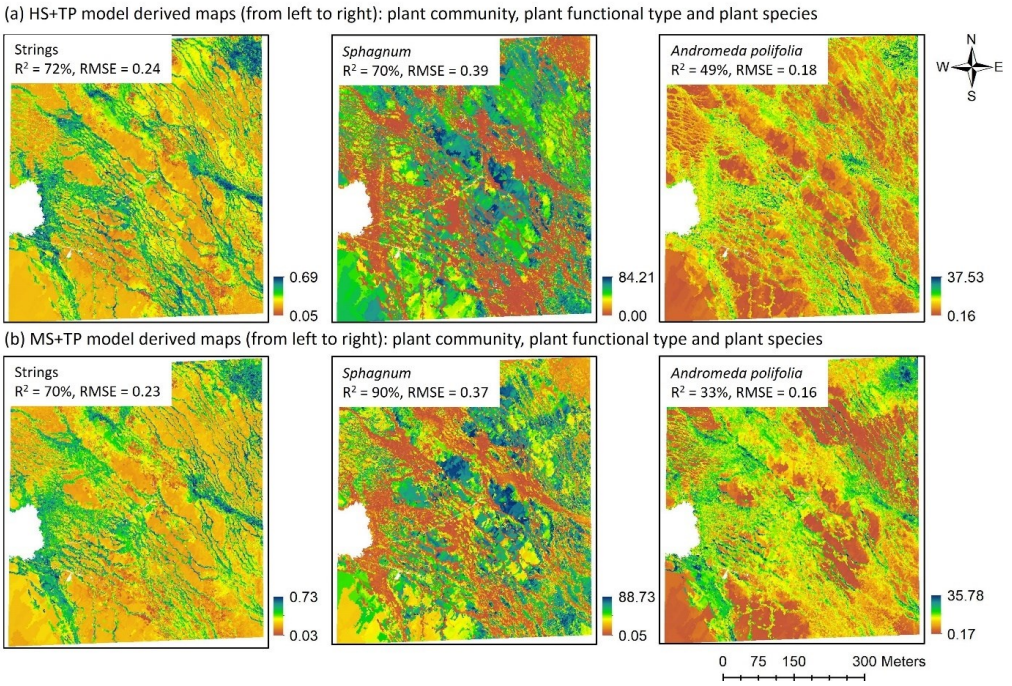


Figure 11 Examples of vegetation maps based on (a) HS+TP and (b) MS+TP models in Halssiaapa. R^2 refers to the percentage of variance explained.

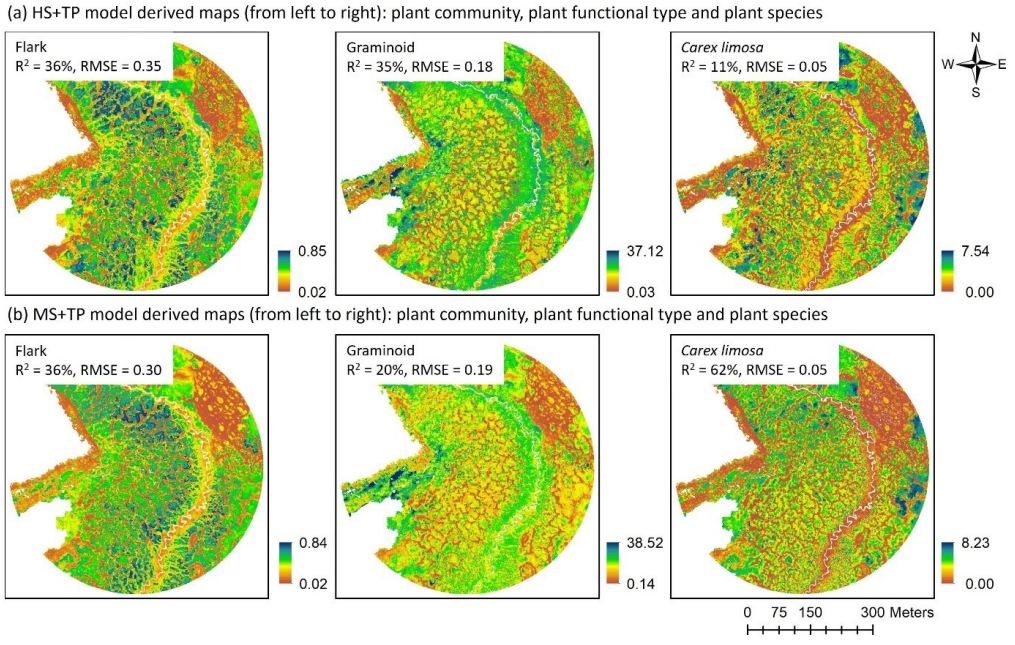


Figure 12 Examples of vegetation maps based on (a) MS+TP and (b) HS+TP models in Kaamanen. R^2 refers to the percentage of variance explained.

3.3 Spatio-temporal patterns of peatland AGB and LAI (Paper III)

The landscape-level AGB and LAI displayed unimodal seasonality, with S2-derived peaks occurring approximately two weeks later than those observed in field measurements (Figure 13). Specifically, the seasonal development of the ground layer AGB and LAI varied among vegetation community types, with forests exhibiting relatively slight seasonal dynamics in AGB and LAI, whereas peatlands showed greater fluctuations (Figure 14).

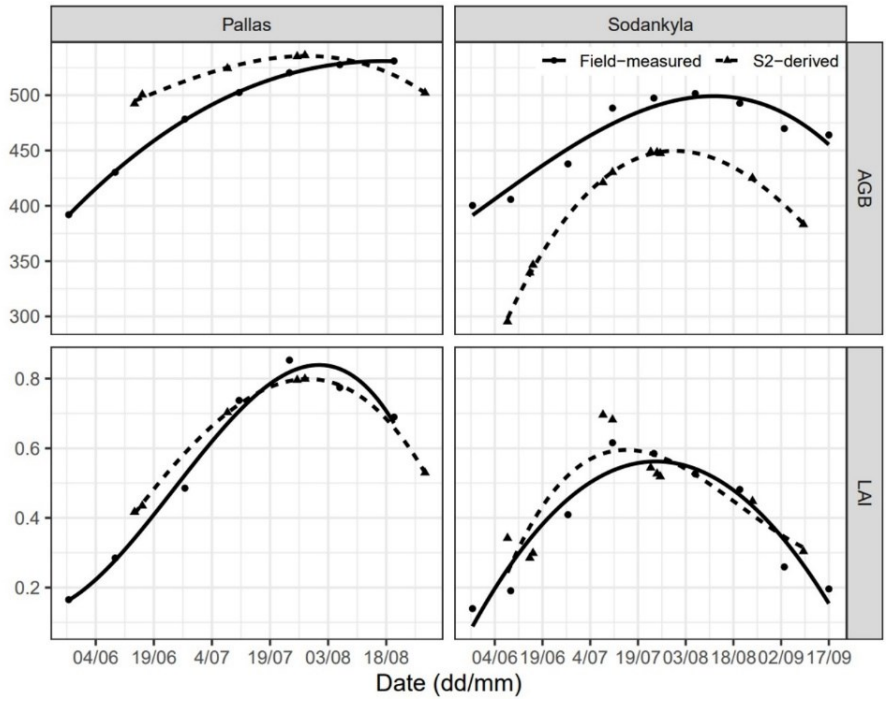


Figure 13 Comparison between field-measured and S2-derived seasonal development of AGB (g m^{-2}) and LAI

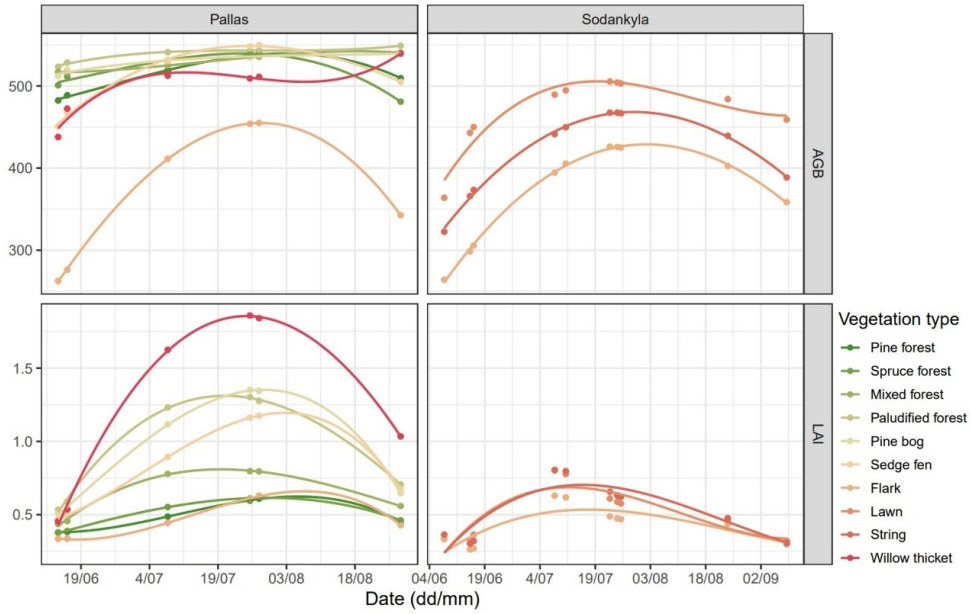


Figure 14 S2-derived seasonal developments of AGB (g m^{-2}) and LAI by vegetation community types

Across the landscape in Pallas, the ground layer AGB and LAI of most forest vegetation remained stable across seasons and differed spatially from those of peatland vegetation, especially in July. Only in the southeastern corner, moist spruce forests with more forbs in the ground layer showed noticeable seasonal variations, with AGB and LAI levels being low in June and reaching maximum levels in late July (Figure 15).

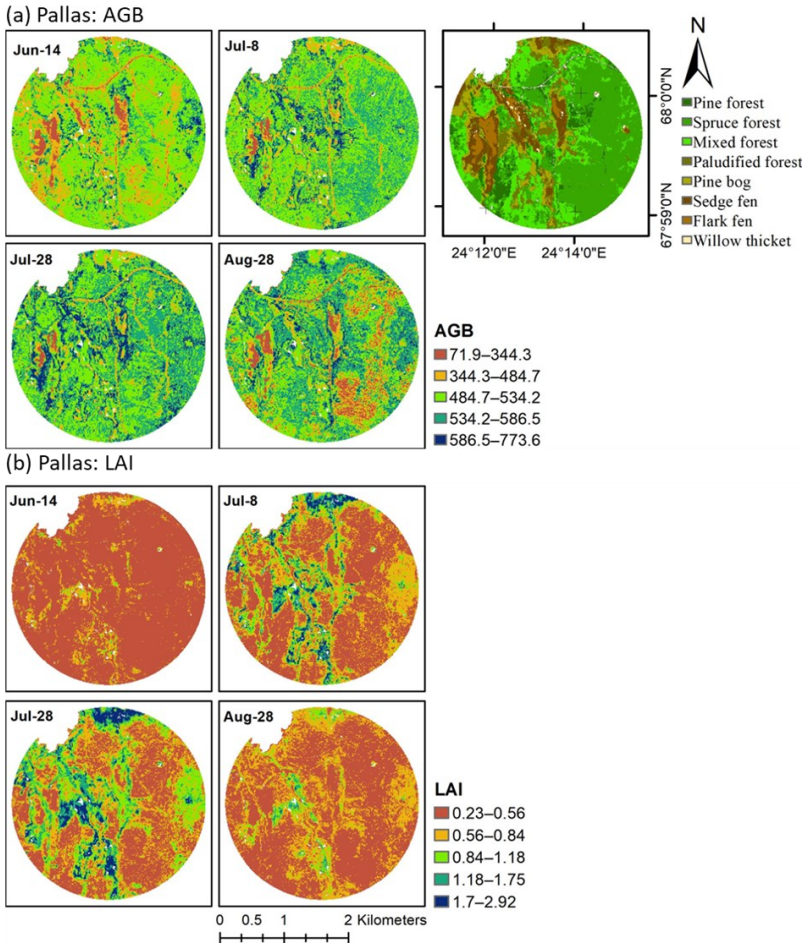


Figure 15 Landscape maps derived from time-series S2 datasets (with 10-m spatial resolution) of (a) ground layer AGB (g m^{-2}), (b) ground layer LAI, and (c) land cover map in Pallas.

In Sodankylä, the spatial and temporal patterns of the AGB and LAI varied among the three vegetation types (Figure 16). For example, flark vegetation typically exhibits lower AGB and LAI values than lawn and string vegetation during the same growth period. However, regarding seasonal changes, AGB displayed distinct trends among vegetation communities, whereas LAI showed nearly uniform trends across the landscape before July.

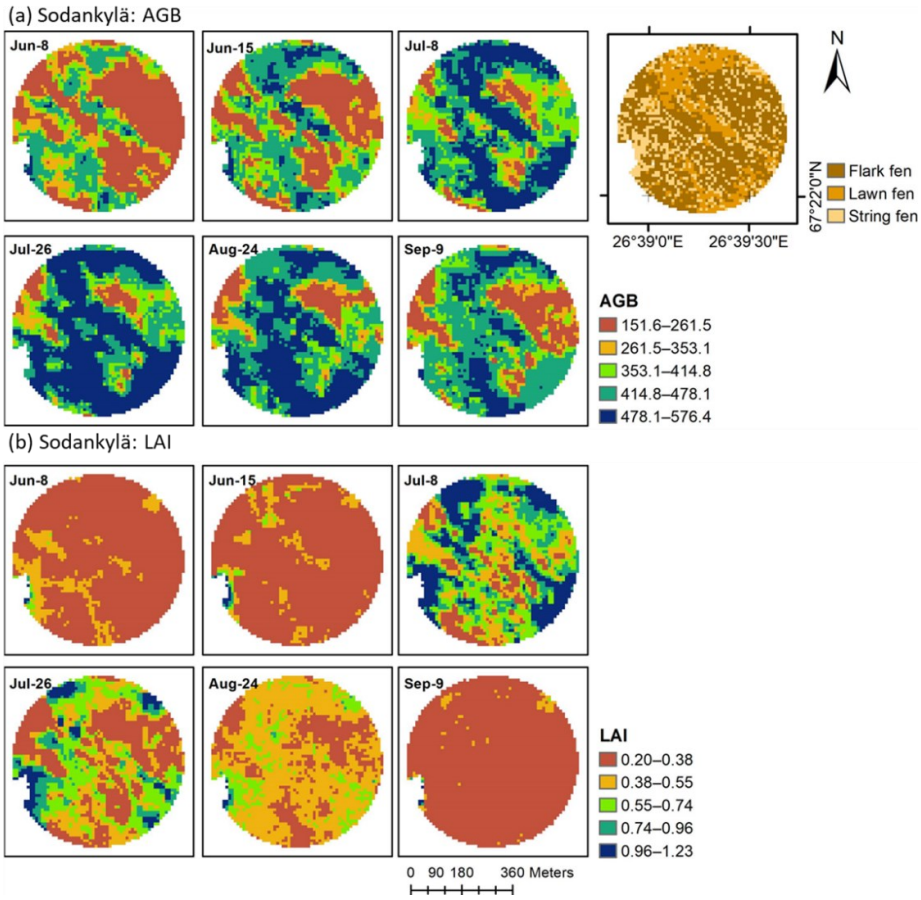


Figure 16 Landscape maps derived from time-series S2 datasets (with 10-m spatial resolution) of (a) ground layer AGB (g m^{-2}), (b) ground layer LAI, and (c) land cover map in Sodankylä.

4 Discussion

4.1 The benefits of multi-temporal RS data for detecting peatland vegetation (Papers I and III)

Paper I indicated that whole-season models outperformed single-date models in predicting various peatland vegetation characteristics (Figure 3 and Figure 4). This finding aligns with those of previous studies, highlighting the added value of multi-temporal spectral data for vegetation mapping applications (Dudley et al., 2015, Arroyo-Mora et al., 2018).

The performance of single-date models fluctuates widely, possibly because of a mixture of spectral signatures that represent the plant composition within a field plot, limiting the detectability of specific vegetation characteristics (McPartland et al., 2019). Vegetation phenology poses another challenge to individual date-based models, as variations in phenology of different plants and communities can impact their visibility and spectral properties. In addition, hydrological conditions of the peatlands vary seasonally. As a result, these relationships with vegetation communities vary over time (Cole et al., 2014b), suggesting that multi-temporal data are more likely to ensure better modelling.

Certain periods (e.g., mid-July–August) demonstrated the potential to achieve acceptable explained variance rates for detecting plant communities and predicting the vegetation cover. However, no specific narrow temporal windows were identified for predicting vegetation AGB and LAI (Figure 3 and Figure 4, **Paper I**). For instance, if the timing of the single-date model coincides with a critical period in the vegetation growth cycle, such as the peak of the growing season, it increases the chance of capturing relevant vegetation information (Cole et al., 2014b, Dudley et al., 2015). Supported by this finding, **Paper II** conducted UAV campaigns during the last week of July, promising the generation of peatland vegetation maps from plant communities and PFTs to plant species.

Vegetation AGB and LAI differ among vegetation types and are affected by factors other than 2D vegetation cover and plant composition, such as structural complexity and vegetation layering, thus hindering a good interpretation of RS spectral signatures (Onodi et al., 2017). Nevertheless, employing multi-temporal RS

regression models can help mitigate these challenges by incorporating additional information related to vegetation seasonality. **Paper III** demonstrates the effectiveness of time-series S2 datasets in predicting field-measured field layer vegetation AGB and LAI (Figure 5) and producing a series of landscape level maps (Figure 15 and Figure 16).

4.2 The role of HS features in peatland vegetation mapping (Papers I and II)

Paper I revealed that a spectral resolution of 20 nm primarily ensured the high variance explained compared to coarser spectral resolution options and S2A band simulations. However, this does not necessarily mean that the spectral resolution should be as high as possible to achieve the best outputs (Figure 6 and Figure 7). Some studies have reported the potential advantages of HS data in quantitatively deriving vegetation characteristics, such as plant biophysics and species classification (Hennessy et al., 2020, Bradter et al., 2020). However, others have also argued that the spectral resolution might not need to be high (e.g., 1–10 nm) because hundreds of spectral bands can introduce redundant information, leading to the implementation of dimensional reduction processes typically applied to HS data (Kale et al., 2017, Morales et al., 2021).

The UAV-based regressions showed that the contribution of UAV HS features was not as significant as expected for peatland vegetation mapping, and no single type of UAV data combination consistently outperformed the others across various vegetation variables (Figure 8, **Paper II**). On the other hand, several studies have reported promising results on UAV HS-based vegetation mapping, such as delineating plant communities (Du et al., 2021, Szporak-Wasilewska et al., 2021). However, in **Paper II**, the UAV HS models failed to generate significantly better results than the MS-based models; in some cases, the HS models performed even worse (Figure 9). Echoing **Paper I**, although HS data provide a larger number of narrow spectral bands throughout the spectrum, they did not consistently yield the best modelling performance. This may be due to the high dimensionality and associated noise, hindering rather than facilitating small-scale vegetation spectral separation, particularly in peatland environments (Hennessy et al., 2020, Adam et al., 2010).

In general, the MS models were likely to produce an acceptable percentage of explained variance, whereas the HS models sometimes performed well (Figure 9,

Paper II). Many studies have reported the great potential of using UAV MS data to map vegetation in wetlands (Zhou et al., 2021, Dale et al., 2020) and tundra (Assmann et al., 2019, Fraser et al., 2016), along with reports indicating no significant differences between UAV MS and HS in distinguishing tundra grass species (Kupkova et al., 2023). HS models were valuable in some cases, such as in producing the highest variance explained rates for *Trichophorum* sp. and other individual plant species. This case is consistent with a previous study showing that UAV HS data improved the prediction of two graminoid species (Arasumani et al., 2023). Moreover, some HS bands and indices were found to be more important in the regressions (Figure 10, **Paper II**), and the contributions of specific HS features have been reported elsewhere, such as aiding in mapping wetland habitat types (Szporak-Wasilewska et al., 2021) and plant communities (Du et al., 2021).

Overall, the contribution of HS RS to peatland vegetation mapping is limited, as a spectral resolution of 20 nm and UAV MS RS can yield satisfactory results. Therefore, the use of UAV HS data is not highly recommended considering the trade-offs between the benefits and costs involved in capturing and processing the data, as large high resolution data sets are heavy to process and analyse, taking more time and work than lower resolution data analysis.

4.3 Detectability of spatial and temporal patterns of peatland vegetation characteristics (Papers I–III)

Papers I–III extensively examined the detectability and mappability of various peatland vegetation characteristics using different RS data, thereby providing a comprehensive picture of data usage and vegetation applications.

Generally, the vegetation characteristics of plant communities and PFTs were better predicted than that of individual plant species, a finding supported by existing studies that indicate the viability of spectral detectability among vegetation variables (Steenvoorden et al., 2023, Arasumani et al., 2023, Beyer et al., 2019, Harris et al., 2015). As the proportion of the individual species in community is generally lower than PFTs, it is logical that PFTs are better identifiable. Plant communities and PFTs also represent groups of species that often have coherent and discernible spectral signatures, facilitating their identification and mapping using RS data (Harris et al., 2015, Rebelo et al., 2018, Schweiger et al., 2017, Kattenborn et al., 2019).

Moreover, aggregating data at the level of plant communities or PFTs can provide greater statistical power for modelling and analysis compared to individual species, especially in cases where sample sizes for individual species may be limited (Millard and Richardson, 2015). To elaborate, flarks (wherein wet brown mosses were dominant) and lawns (e.g., *Sphagnum* dominated) were well-recognised spectrally, likely because of their relatively uniform plant species compositions and fewer vegetation layers (Figure 3 and Figure 9). Moreover, higher variance explained rates were observed for *Sphagnum*, evergreen shrubs, and forbs, whereas graminoids appeared to be more challenging (Figure 3 and Figure 9), possibly because of their thin leaves and often relatively low coverage percentages (Lopatin et al., 2017). Individual plant species are often sparsely distributed in small patches, and in some cases, exhibit only subtle spectral differences, leading to poor spectral differentiation (Figure 9), a phenomenon also reported in previous studies (Bertacchi et al., 2019, Lopatin et al., 2017, Dudley et al., 2015).

UAV-derived maps effectively captured spatial patterns across different types of heterogeneity at two sites: linear strings in Halssiaapa and string mazes in Kaamanen (Figure 11 and Figure 12). Local variations in vegetation cover allowed wet brown mosses and *Sphagnum* to be accurately mapped in Halssiaapa, while feather mosses were more precisely depicted in Kaamanen. This demonstrates the value of UAV data for peatland vegetation mapping, particularly when integrated with topographical features.

Furthermore, **Papers I and III**, based on time-series RS datasets, demonstrated that vegetation presents different seasonality among PFTs and community types. Single-date spectroscopy regressions (Figure 4) showed that the spectral detectability of vegetation AGB and LAI varied significantly depending on the date. In addition, the time-series S2 datasets successfully constructed regression models to estimate field-measured vegetation AGB and LAI, explaining 24–50% and 49–56% of the variance, respectively (Figure 5). This performance is comparable to that of earlier studies. For example, in S2-based landscape mapping, AGB was explained by 36–70% (Räsänen et al., 2021) and LAI by 75–89% (Amin et al., 2018). Similarly, in S2-based seasonal dynamic models, Wang et al. (2019) obtained explained variances of 9–41% for AGB and 36–58% for LAI. Nevertheless, the S2 models performed poorly in forest community types with very high AGB and LAI values (Figure 13), possibly

because tree crowns hinders the ability of the ground layer S2 models to capture ground vegetation effectively (Wang et al., 2022, Fassnacht et al., 2021).

Additionally, for some very low AGB and LAI values in peatlands, S2 datasets might not possess sufficient spatial and spectral resolution to capture the nuances of vegetation structure and function, resulting in relatively poor modelling. As demonstrated in **Paper I**, the low spectral detectability of AGB and LAI was observed before July or late August (Figure 4). During these periods, RS signatures are less correlated with vegetation parameters due to the presence of non-photosynthetic structures such as flowers, stems, seed heads, and senescent/dead parts, which interfere with ground reflectance (Beamish et al., 2017, Tian et al., 2021). Especially in the early season there often is more flooding also impacting detectability of vegetation parameters.

AGB and LAI followed similar unimodal seasonality, but there was a 21-day gap for AGB and a 10-day gap for LAI at the phenological peak between the field measurements and S2 estimations (Figure 13). Other studies have also reported phenological differences between field and S2 values with periods of 8–30 days (Tian et al., 2021, Vrieling et al., 2018, Garisoain et al., 2023, Linkosalmi et al., 2022). One study demonstrated a high correlation between S2 spectra and field measurements in the same period (Arroyo-Mora et al., 2018), whereas in this case study, an 8-day initial time difference between the S2 image acquisition date and the field inventory date was used to build the time series S2 dataset. Furthermore, in the field, vegetation inventories were recorded by visual interpretation of individual plants within the 0.25 m^2 plot. However, S2 predictors were based on a 10 m spatial resolution pixel that included mixed reflectance signatures of all land cover, causing obvious uncertainties between field observations and S2 estimations.

The series of S2-derived maps illustrates the spatio-temporal patterns of AGB and LAI across boreal landscapes (Figure 14–Figure 16). Specifically, peatland vegetation communities exhibited distinct seasonal trajectories in AGB and LAI, whereas forests demonstrated relatively stable variations in ground layer AGB and LAI. These maps reinforce previous findings that S2 data are effective in predicting landscape AGB and LAI (Räsänen et al., 2020, Majasalmi and Rautiainen, 2016) and tracking vegetation

phenology (Misra et al., 2020, Arroyo-Mora et al., 2018), particularly in treeless peatlands.

4.4 Limitations and future research

This thesis comprehensively examines the use of various RS data for monitoring peatland vegetation, revealing the advantages of different RS data for specific vegetation characteristics. However, some issues need to be considered. First, the study sites were limited to northern pristine peatlands, while disturbed and restored sites were not examined. To date, more than 25% of peatlands in Europe have been degraded (Tanneberger et al., 2021); in Finland, this figure has reached 50% (Turunen and Valpola, 2020). Previous studies have reported that drainage ditches decrease plant diversity and alter plant composition within peatlands (Gatis et al., 2016). Restoration measures, such as rewetting, aim to facilitate the succession of degraded peatlands towards a pristine-like status, where vegetation cover can serve as an indicator of ecosystem recovery (Haapalehto et al., 2017, Kyrkjeeide et al., 2024). Moreover, hydrological processes play a crucial role in shaping the vegetation dynamics of peatlands. Coupling hydrological models with vegetation growth models can provide valuable insights into how changes in water availability influence vegetation dynamics and vice versa. However, the interaction between vegetation ecology and hydrology, and the impact of interaction on different peatland types has not been fully studied within the framework of employing RS data (Linkeviciene et al., 2023, Suárez et al., 2024).

Second, although this thesis focuses on three vegetation characteristics—vegetation cover, AGB, and LAI—other plant functional traits also have value for further research. Researchers have highlighted other properties, such as photosynthetic pathways and activity, plant height, and nitrogen and phosphorous content, which interact with topography, soil, and geodiversity. These traits can be remotely sensed and utilised to characterise ecosystem conditions, including vitality, stress, processes, disturbances, and resource limitations (Lausch et al., 2024). Moreover, there is a growing trend towards developing process-based models to comprehensively understand peatland dynamics, with extensive integration of vegetation information (Mozafari et al., 2023). This trend also encourages innovation in physically based

models by incorporating RS methods to represent the sophisticated spatial variability and dynamics of peatland vegetation with diverse characteristics.

Third, the case studies primarily utilised optical passive RS data, with only active RS data being the LiDAR-derived TP features used in **Paper II**. However, other active RS data, such as Synthetic Aperture Radar (SAR) and interferometric SAR (InSAR) data, were not used. Leveraging the advantages of independence from natural light sources and fewer time constraints, active RS techniques are increasingly being used to monitor peatland conditions, focusing primarily on hydrological functions and subsidence (Minasny et al., 2023). However, they also provide valuable insights into vegetation density, biomass, and structure, although further investigation is required (Abdelmajeed and Juszczak, 2024). Moreover, typical active RS data are collected via satellites with a coarser spatial resolution (5–40 m), whereas trade-offs between operation costs and missions limit the prevalence of airborne SAR. Therefore, future research should investigate the use of multi-source active and passive RS data, such as integrating data at different spatial resolutions. For instance, a recent publication reported a successful trial for classifying peatland subclasses by combining Landsat-7 MS, SAR, and InSAR data (Pontone et al., 2024).

5 Conclusions

This thesis explores the utilisation of diverse RS data to delineate the spatial patterns of peatland vegetation and monitor their phenology across the three northern peatlands. This elucidates the advantages of three types of RS data: seasonal spectroscopy data for conducting various spectral analyses at the plot level, UAV images for precise vegetation mapping, and time-series S2 datasets for tracking vegetation phenology in northern treeless landscapes. Multi-temporal RS data not only facilitate the detection of various vegetation characteristics, but also enable tracing of their seasonal developments. In the absence of seasonal data, individual periods (e.g., mid-July–August) could be useful for vegetation mapping. Surprisingly, ultra-high spectral resolution (i.e., 1–10 nm) and HS features are not as crucial as anticipated in aiding vegetation detection. Instead, UAV MS and S2 satellite data performed well. Moreover, S2 regression models revealed spatio-temporal patterns of vegetation AGB and LAI, particularly demonstrating their efficacy in treeless peatlands and elaborating on vegetation phenology among vegetation types. Overall, these studies suggest that peatland vegetation can be more reliably characterised at the community and PFT levels through RS data rather than at the plant species level. Specifically, vegetation communities and vegetation cover could be mapped using UAV imagery over a single period, and time-series S2 satellite datasets showed promising results in tracking seasonal trajectories of vegetation AGB and LAI in treeless peatlands.

This thesis underscores the complexity of applying RS in peatland monitoring, where certain methods prove effective under specific conditions, while others do not. The heterogeneous microtopography and varied vegetation cover of surfaces within a single peatland and large differences between peatland sites emphasize the need for tailored RS approaches. Therefore, it is not feasible to design a simple or universally applicable RS data strategy for peatlands. In general, the results suggest the advantages of multi-temporal RS data and high spatial resolution UAV data, while the benefits of HS data appear to be more limited. This new understanding indicates that researchers and practitioners should carefully prioritize the selection and integration of multi-temporal and high-resolution RS data to meet specific research objectives.

In light of these findings, I recommend a multifaceted approach that combines UAV spectral data with additional topographic information to improve the accuracy and applicability of RS in peatland studies. Future developments in this field could focus on overcoming challenges posed by high dimensionality and noise in HS data, potentially through the development of advanced algorithms and artificial intelligence techniques specifically tailored to peatlands. By addressing these challenges, RS could become a more reliable and powerful tool for peatland conservation and management.

References

ABDELMAJEED, A. Y. A. & JUSZCZAK, R. 2024. Challenges and Limitations of Remote Sensing Applications in Northern Peatlands: Present and Future Prospects. *Remote Sensing,* 16**,** 591.

ADAM, E., MUTANGA, O. & RUGEGE, D. 2010. Multispectral and hyperspectral remote sensing for identification and mapping of wetland vegetation: a review. *Wetlands Ecology and Management,* 18**,** 281-296.

AMIN, E., VERRELST, J., RIVERA-CAICEDO, J. P., PASQUALOTTO, N., DELEGIDO, J., VERDU, A. R. & MORENO, J. 2018. The Sensagri Sentinel-2 Lai Green and Brown Product: From Algorithm Development Towards Operational Mapping. *Igarss 2018 - 2018 Ieee International Geoscience and Remote Sensing Symposium***,** 1822-1825.

ANDERSEN, R., POULIN, M., BORCARD, D., LAIHO, R., LAINE, J., VASANDER, H. & TUITTILA, E. T. 2011. Environmental control and spatial structures in peatland vegetation. *Journal of Vegetation Science,* 22**,** 878-890.

ARASUMANI, M., THIEL, F., PHAM, V. D., HELLMANN, C., KAISER, M. & VAN DER LINDEN, S. 2023. Advancing peatland vegetation mapping by spaceborne imaging spectroscopy. *Ecological Indicators,* 154.

ARROYO-MORA, J. P., KALACSKA, M., SOFFER, R., IFIMOV, G., LEBLANC, G., SCHAAF, E. S. & LUCANUS, O. 2018. Evaluation of phenospectral dynamics with Sentinel-2A using a bottom-up approach in a northern ombrotrophic peatland. *Remote Sensing of Environment,* 216**,** 544-560.

ASSIRI, M., SARTORI, A., PERSICHETTI, A., MIELE, C., FAELGA, R. A., BLOUNT, T. & SILVESTRI, S. 2023. Leaf area index and aboveground biomass estimation of an alpine peatland with a UAV multi-sensor approach. *Giscience & Remote Sensing,* 60.

ASSMANN, J. J., KERBY, J. T., CUNLIFFE, A. M. & MYERS-SMITH, I. H. 2019. Vegetation monitoring using multispectral sensors - best practices and lessons learned from high latitudes. *Journal of Unmanned Vehicle Systems,* 7**,** 54-75.

AURELA, M., LOHILA, A., TUOVINEN, J. P., HATAKKA, J., PENTTILA, T. & LAURILA, T. 2015. Carbon dioxide and energy flux measurements in four northern-boreal ecosystems at Pallas. *Boreal Environment Research,* 20**,** 455-473.

BAATZ, M. & SCHÄPE, A. Multiresolution Segmentation: an optimization approach for high quality multi-scale image segmentation. 2000. 12-23.

BEAMISH, A. L., COOPS, N., CHABRILLAT, S. & HEIM, B. 2017. A Phenological Approach to Spectral Differentiation of Low-Arctic Tundra Vegetation Communities, North Slope, Alaska. *Remote Sensing,* 9.

BERHANE, T. M., LANE, C. R., WU, Q. S., ANENKHONOV, O. A., CHEPINOGA, V. V., AUTREY, B. C. & LIU, H. X. 2018. Comparing Pixel- and Object-Based Approaches in Effectively Classifying Wetland-Dominated Landscapes. *Remote Sensing,* 10.

BERTACCHI, A., GIANNINI, V., DI FRANCO, C. & SILVESTRI, N. 2019. Using unmanned aerial vehicles for vegetation mapping and identification of botanical species in wetlands. *Landscape and Ecological Engineering,* 15**,** 231-240.

BEYER, F., JURASINSKI, G., COUWENBERG, J. & GRENZDORFFER, G. 2019. Multisensor data to derive peatland vegetation communities using a fixed-wing unmanned aerial vehicle. *International Journal of Remote Sensing,* 40**,** 9103-9125.

BLASCHKE, T., HAY, G. J., KELLY, M., LANG, S., HOFMANN, P., ADDINK, E., FEITOSA, R. Q., VAN DER MEER, F., VAN DER WERFF, H., VAN COILLIE, F. & TIEDE, D. 2014. Geographic Object-Based Image Analysis - Towards a new paradigm. *Isprs Journal of Photogrammetry and Remote Sensing,* 87**,** 180-191.

BRADTER, U., O'CONNELL, J., KUNIN, W. E., BOFFEY, C. W. H., ELLIS, R. J. & BENTON, T. G. 2020. Classifying grass-dominated habitats from remotely sensed data: The influence of spectral resolution, acquisition time and the vegetation classification system on accuracy and thematic resolution. *Science of the Total Environment,* 711.

BREIMAN, L. 2001. Random forests. *Machine Learning,* 45**,** 5-32.

BUBIER, J. L., ROCK, B. N. & CRILL, P. M. 1997. Spectral reflectance measurements of boreal wetland and forest mosses. *Journal of Geophysical Research-Atmospheres,* 102**,** 29483-29494.

CHEN, J. M. & BLACK, T. A. 1992. Defining Leaf-Area Index for Non-Flat Leaves. *Plant Cell and Environment,* 15**,** 421-429.

COLE, B., MCMORROW, J. & EVANS, M. 2014a. Empirical Modelling of Vegetation Abundance from Airborne Hyperspectral Data for Upland Peatland Restoration Monitoring. *Remote Sensing,* 6**,** 716-739.

COLE, B., MCMORROW, J. & EVANS, M. 2014b. Spectral monitoring of moorland plant phenology to identify a temporal window for hyperspectral remote sensing of peatland. *Isprs Journal of Photogrammetry and Remote Sensing,* 90**,** 49-58.

COUWENBERG, J., THIELE, A., TANNEBERGER, F., AUGUSTIN, J., BÄRISCH, S., DUBOVIK, D., LIASHCHYNSKAYA, N., MICHAELIS, D., MINKE, M., SKURATOVICH, A. & JOOSTEN, H. 2011. Assessing greenhouse gas emissions from peatlands using vegetation as a proxy. *Hydrobiologia,* 674**,** 67-89.

CZAPIEWSKI, S. & SZUMINSKA, D. 2022. An Overview of Remote Sensing Data Applications in Peatland Research Based on Works from the Period 2010-2021. *Land,* 11.

DALE, J., BURNSIDE, N. G., HILL-BUTLER, C., BERG, M. J., STRONG, C. J. & BURGESS, H. M. 2020. The Use of Unmanned Aerial Vehicles to Determine Differences in Vegetation Cover: A Tool for Monitoring Coastal Wetland Restoration Schemes. *Remote Sensing,* 12.

DAVIDSON, S. J., GOUD, E. M., MALHOTRA, A., ESTEY, C. O., KORSAH, P. & STRACK, M. 2021. Linear Disturbances Shift Boreal Peatland Plant Communities Toward Earlier Peak Greenness. *Journal of Geophysical Research-Biogeosciences,* 126.

DIELEMAN, C. M., BRANFIREUN, B. A. & LINDO, Z. 2017. Northern peatland carbon dynamics driven by plant growth form - the role of graminoids. *Plant and Soil,* 415**,** 25-35.

DINSMORE, K. J., DREWER, J., LEVY, P. E., GEORGE, C., LOHILA, A., AURELA, M. & SKIBA, U. M. 2017. Growing season CH4 and N2O fluxes from a subarctic landscape in northern Finland; from chamber to landscape scale. *Biogeosciences,* 14**,** 799-815.

DRONOVA, I., KISLIK, C., DINH, Z. & KELLY, M. 2021. A Review of Unoccupied Aerial Vehicle Use in Wetland Applications: Emerging Opportunities in Approach, Technology, and Data. *Drones,* 5.

DU, B. J., MAO, D. H., WANG, Z. M., QIU, Z. Q., YAN, H. Q., FENG, K. D. & ZHANG, Z. B. 2021. Mapping Wetland Plant Communities Using Unmanned Aerial

Vehicle Hyperspectral Imagery by Comparing Object/Pixel-Based Classifications Combining Multiple Machine-Learning Algorithms. *Ieee Journal of Selected Topics in Applied Earth Observations and Remote Sensing,* 14**,** 8249-8258.

DUDLEY, K. L., DENNISON, P. E., ROTH, K. L., ROBERTS, D. A. & COATES, A. R. 2015. A multi-temporal spectral library approach for mapping vegetation species across spatial and temporal phenological gradients. *Remote Sensing of Environment,* 167**,** 121-134.

ERUDEL, T., FABRE, S., HOUET, T., MAZIER, F. & BRIOTTET, X. 2017. Criteria Comparison for Classifying Peatland Vegetation Types Using In Situ Hyperspectral Measurements. *Remote Sensing,* 9.

FASSNACHT, F. E., POBLETE-OLIVARES, J., RIVERO, L., LOPATIN, J., CEBALLOS-COMISSO, A. & GALLEGUILLOS, M. 2021. Using Sentinel-2 and canopy height models to derive a landscape-level biomass map covering multiple vegetation types. *International Journal of Applied Earth Observation and Geoinformation,* 94.

FRASER, R. H., OLTHOF, I., LANTZ, T. C. & SCHMITT, C. 2016. UAV photogrammetry for mapping vegetation in the low-Arctic. *Arctic Science,* 2**,** 79-102.

GARISOAIN, R., DELIRE, C., DECHARME, B., FERRANT, S., GRANOUILLAC, F., PAYRE-SUC, V. & GANDOIS, L. 2023. A Study of Dominant Vegetation Phenology in a *Sphagnum* Mountain Peatland Using In Situ and Sentinel-2 Observations. *Journal of Geophysical Research-Biogeosciences,* 128.

GATIS, N., LUSCOMBE, D. J., GRAND-CLEMENT, E., HARTLEY, I. P., ANDERSON, K., SMITH, D. & BRAZIER, R. E. 2016. The effect of drainage ditches on vegetation diversity and CO_2 fluxes in a *Molinia caerulea*-dominated peatland. *Ecohydrology,* 9**,** 407-420.

GOUD, E. M., MOORE, T. R. & ROULET, N. T. 2017. Predicting peatland carbon fluxes from non-destructive plant traits. *Functional Ecology,* 31**,** 1824-1833.

HAAPALEHTO, T., JUUTINEN, R., KAREKSELA, S., KUITUNEN, M., TAHVANAINEN, T., VUORI, H. & KOTIAHO, J. S. 2017. Recovery of plant communities after ecological restoration of forestry-drained peatlands. *Ecology and Evolution,* 7**,** 7848-7858.

HARRIS, A., CHARNOCK, R. & LUCAS, R. M. 2015. Hyperspectral remote sensing of peatland floristic gradients. *Remote Sensing of Environment,* 162**,** 99-111.

HENGL, T., NUSSBAUM, M., WRIGHT, M. N., HEUVELINK, G. B. M. & GRALER, B. 2018. Random forest as a generic framework for predictive modeling of spatial and spatio-temporal variables. *Peerj,* 6.

HENNESSY, A., CLARKE, K. & LEWIS, M. 2020. Hyperspectral Classification of Plants: A Review of Waveband Selection Generalisability. *Remote Sensing,* 12.

HOSSAIN, M. D. & CHEN, D. 2019. Segmentation for Object-Based Image Analysis (OBIA): A review of algorithms and challenges from remote sensing perspective. *Isprs Journal of Photogrammetry and Remote Sensing,* 150**,** 115-134.

HUGELIUS, G., LOISEL, J., CHADBURN, S., JACKSON, R. B., JONES, M., MACDONALD, G., MARUSHCHAK, M., OLEFELDT, D., PACKALEN, M., SIEWERT, M. B., TREAT, C., TURETSKY, M., VOIGT, C. & YU, Z. C. 2020. Large stocks of peatland carbon and nitrogen are vulnerable to permafrost thaw. *Proceedings of the National Academy of Sciences of the United States of America,* 117**,** 20438-20446.

JAFARZADEH, H., MAHDIANPARI, M., GILL, E. W., BRISCO, B. & MOHAMMADIMANESH, F. 2022. Remote Sensing and Machine Learning Tools to Support Wetland Monitoring: A Meta-Analysis of Three Decades of Research. *Remote Sensing,* 14.

JUNTTILA, S., KELLY, J., KLJUN, N., AURELA, M., KLEMEDTSSON, L., LOHILA, A., NILSSON, M. B., RINNE, J., TUITTILA, E. S., VESTIN, P., WESLIEN, P. & EKLUNDH, L. 2021. Upscaling Northern Peatland CO2 Fluxes Using Satellite Remote Sensing Data. *Remote Sensing,* 13.

JUUTINEN, S., VIRTANEN, T., KONDRATYEV, V., LAURILA, T., LINKOSALMI, M., MIKOLA, J., NYMAN, J., RASANEN, A., TUOVINEN, J. P. & AURELA, M. 2017. Spatial variation and seasonal dynamics of leaf-area index in the arctic tundra-implications for linking ground observations and satellite images. *Environmental Research Letters,* 12.

KALE, K. V., SOLANKAR, M. M., NALAWADE, D. B., DHUMAL, R. K. & GITE, H. R. 2017. A Research Review on Hyperspectral Data Processing and Analysis Algorithms. *Proceedings of the National Academy of Sciences India Section a-Physical Sciences,* 87**,** 541-555.

KATTENBORN, T., FASSNACHT, F. E. & SCHMIDTLEIN, S. 2019. Differentiating plant functional types using reflectance: which traits make the difference? *Remote Sensing in Ecology and Conservation,* 5**,** 5-19.

KIMMEL, K. & MANDER, Ü. 2010. Ecosystem services of peatlands: Implications for restoration. *Progress in Physical Geography-Earth and Environment,* 34**,** 491-514.

KOEBSCH, F., SONNENTAG, O., JARVEOJA, J., PELTONIEMI, M., ALEKSEYCHIK, P., AURELA, M., ARSLAN, A. N., DINSMORE, K., GIANELLE, D., HELFTER, C., JACKOWICZ-KORCZYNSKI, M., KORRENSALO, A., LEITH, F., LINKOSALMI, M., LOHILA, A., LUND, M., MADDISON, M., MAMMARELLA, I., MANDER, U., MINKKINEN, K., PICKARD, A., PULLENS, J. W. M., TUITTILA, E. S., NILSSON, M. B. & PEICHL, M. 2020. Refining the role of phenology in regulating gross ecosystem productivity across European peatlands. *Global Change Biology,* 26**,** 876-887.

KORPELA, I., HAAPANEN, R., KORRENSALO, A., TUITTILA, E. S. & VESALA, T. 2020. Fine-resolution mapping of microforms of a boreal bog using aerial images and waveform-recording LiDAR. *Mires and Peat,* 26.

KORRENSALO, A., MEHTATALO, L., ALEKSEYCHIK, P., ULJAS, S., MAMMARELLA, I., VESALA, T. & TUITTILA, E. S. 2020. Varying Vegetation Composition, Respiration and Photosynthesis Decrease Temporal Variability of the CO2 Sink in a Boreal Bog. *Ecosystems,* 23**,** 842-858.

KROSS, A. S. E., ROULET, N. T., MOORE, T. R., LAFLEUR, P. M., HUMPHREYS, E. R., SEAQUIST, J. W., FLANAGAN, L. B. & AURELA, M. 2014. Phenology and its role in carbon dioxide exchange processes in northern peatlands. *Journal of Geophysical Research-Biogeosciences,* 119**,** 1370-1384.

KUCHARCZYK, M., HAY, G. J., GHAFFARIAN, S. & HUGENHOLTZ, C. H. 2020. Geographic Object-Based Image Analysis: A Primer and Future Directions. *Remote Sensing,* 12.

KUPKOVA, L., CERVENA, L., POTUCKOVA, M., LYSAK, J., ROUBALOVA, M., HRAZSKY, Z., BREZINA, S., EPSTEIN, H. E. & MULLEROVA, J. 2023. Towards reliable monitoring of grass species in nature conservation: Evaluation of the potential of UAV and PlanetScope multi-temporal data in the Central European tundra. *Remote Sensing of Environment,* 294.

KYRKJEEIDE, M. O., JOKERUD, M., MEHLHOOP, A. C., LUNDE, L. M. F., FANDREM, M. & LYNGSTAD, A. 2024. Peatland restoration in Norway - evaluation of ongoing monitoring and identification of plant indicators of restoration success. *Nordic Journal of Botany*.

LAINE, A. M., BUBIER, J., RIUTTA, T., NILSSON, M. B., MOORE, T. R., VASANDER, H. & TUITTILA, E. S. 2012. Abundance and composition of plant biomass as potential controls for mire net ecosytem CO2 exchange. *Botany,* 90**,** 63-74.

LAUSCH, A., SELSAM, P., PAUSE, M. & BUMBERGER, J. 2024. Monitoring vegetation- and geodiversity with remote sensing and traits. *Philosophical Transactions of the Royal Society a-Mathematical Physical and Engineering Sciences,* 382.

LEIFELD, J., WÜST-GALLEY, C. & PAGE, S. 2019. Intact and managed peatland soils as a source and sink of GHGs from 1850 to 2100. *Nature Climate Change,* 9**,** 945-+.

LEPPÄLÄ, M., KUKKO-OJA, K., LAINE, R. & TUITTILA, E. S. 2008. Seasonal dynamics of CO2 exchange during primary succession of boreal mires as controlled by phenology of plants. *Ecoscience,* 15**,** 460-471.

LINKEVICIENE, R., SIMANAUSKIENE, R., KIBIRKSTIS, G., GRIGAITE, O. & TAMINSKAS, J. 2023. Hydrological and botanical diversity of a raised bog and its evaluation using *in situ* and remote sensing methods. *Journal of Hydrology,* 617.

LINKOSALMI, M., TUOVINEN, J. P., NEVALAINEN, O., PELTONIEMI, M., TANIS, C. M., ARSLAN, A. N., RAINNE, J., LOHILA, A., LAURILA, T. & AURELA, M. 2022. Tracking vegetation phenology of pristine northern boreal peatlands by combining digital photography with CO2 flux and remote sensing data. *Biogeosciences,* 19**,** 4747-4765.

LOPATIN, J., FASSNACHT, F. E., KATTENBORN, T. & SCHMIDTLEIN, S. 2017. Mapping plant species in mixed grassland communities using close range imaging spectroscopy. *Remote Sensing of Environment,* 201**,** 12-23.

MAANAVILJA, L., RIUTTA, T., AURELA, M., PULKKINEN, M., LAURILA, T. & TUITTILA, E. S. 2011. Spatial variation in CO2 exchange at a northern aapa mire. *Biogeochemistry,* 104**,** 325-345.

MAJASALMI, T. & RAUTIAINEN, M. 2016. The potential of Sentinel-2 data for estimating biophysical variables in a boreal forest: a simulation study. *Remote Sensing Letters,* 7**,** 427-436.

MALHOTRA, A., ROULET, N. T., WILSON, P., GIROUX-BOUGARD, X. & HARRIS, L. I. 2016. Ecohydrological feedbacks in peatlands: an empirical test of the relationship among vegetation, microtopography and water table. *Ecohydrology,* 9**,** 1346-1357.

MEINSHAUSEN, N. 2006. Quantile regression forests. *Journal of Machine Learning Research,* 7**,** 983-999.

MILLARD, K. & RICHARDSON, M. 2015. On the Importance of Training Data Sample Selection in Random Forest Image Classification: A Case Study in Peatland Ecosystem Mapping. *Remote Sensing,* 7**,** 8489-8515.

MINASNY, B., ADETSU, D. V., AITKENHEAD, M., ARTZ, R. R. E., BAGGALEY, N., BARTHELMES, A., BEUCHER, A., CARON, J., CONCHEDDA, G., CONNOLLY, J., DERAGON, R., EVANS, C., FADNES, K., FIANTIS, D., GAGKAS, Z., GILET, L., GIMONA, A., GLATZEL, S., GREVE, M. H., HABIB, W., HERGOUALC'H, K., HERMANSEN, C., KIDD, D. B., KOGANTI, T., KOPANSKY, D., LARGE, D. J., LARMOLA, T., LILLY, A., LIU, H. J.,

MARCUS, M., MIDDLETON, M., MORRISON, K., PETERSEN, R. J., QUAIFE, T., ROCHEFORT, L., RUDIYANTO, TOCA, L., TUBIELLO, F. N., WEBER, P. L., WELDON, S., WIDYATMANTI, W., WILLIAMSON, J. & ZAK, D. 2023. Mapping and monitoring peatland conditions from global to field scale. *Biogeochemistry*.

MISRA, G., CAWKWELL, F. & WINGLER, A. 2020. Status of Phenological Research Using Sentinel-2 Data: A Review. *Remote Sensing,* 12.

MOHAMMEDSHUM, A. A. & KOOISTRA, L. 2015. Mapping tree distribution and LAI in peatlands using field methods and imaging spectroscopy: a case study for the Haaksbergerveen, the Netherlands. *International Journal of Remote Sensing,* 36**,** 4535-4549.

MORALES, G., SHEPPARD, J. W., LOGAN, R. D. & SHAW, J. A. 2021. Hyperspectral Dimensionality Reduction Based on Inter-Band Redundancy Analysis and Greedy Spectral Selection. *Remote Sensing,* 13.

MOZAFARI, B., BRUEN, M., DONOHUE, S., RENOU-WILSON, F. & O'LOUGHLIN, F. 2023. Peatland dynamics: A review of process-based models and approaches. *Science of the Total Environment,* 877.

NASA. 2024. *What is Remote Sensing?* [Online]. NASA EARTH DATA: NASA EARTH DATA. Available: https://www.earthdata.nasa.gov/learn/backgrounders/remote-sensing [Accessed 11/05/2024].

ONODI, G., KROEL-DULAY, G., KOVACS-LANG, E., ODOR, P., BOTTA-DUKAT, Z., LHOTSKY, B., BARABAS, S., GARADNAI, J. & KERTESZ, M. 2017. Comparing the accuracy of three non-destructive methods in estimating aboveground plant biomass. *Community Ecology,* 18**,** 56-62.

PEICHL, M., GAZOVIC, M., VERMEIJ, I., DE GOEDE, E., SONNENTAG, O., LIMPENS, J. & NILSSON, M. B. 2018. Peatland vegetation composition and phenology drive the seasonal trajectory of maximum gross primary production. *Scientific Reports,* 8.

PONTONE, N., MILLARD, K., THOMPSON, D. K., GUINDON, L. & BEAUDOIN, A. 2024. A hierarchical, multi-sensor framework for peatland sub-class and vegetation mapping throughout the Canadian boreal forest. *Remote Sensing in Ecology and Conservation*.

RÄSÄNEN, A., JUUTINEN, S., KALACSKA, M., AURELA, M., HEIKKINEN, P., MAENPAA, K., RIMALI, A. & VIRTANEN, T. 2020. Peatland leaf-area index and biomass estimation with ultra-high resolution remote sensing. *Giscience & Remote Sensing,* 57**,** 943-964.

RÄSÄNEN, A. & VIRTANEN, T. 2019. Data and resolution requirements in mapping vegetation in spatially heterogeneous landscapes. *Remote Sensing of Environment,* 230.

RÄSÄNEN, A., WAGNER, J., HUGELIUS, G. & VIRTANEN, T. 2021. Aboveground biomass patterns across treeless northern landscapes. *International Journal of Remote Sensing,* 42**,** 4536-4561.

REBELO, A. J., SOMERS, B., ESLER, K. J. & MEIRE, P. 2018. Can wetland plant functional groups be spectrally discriminated? *Remote Sensing of Environment,* 210**,** 25-34.

RUPP, D., KANE, E. S., DIELEMAN, C., KELLER, J. K. & TURETSKY, M. 2019. Plant functional group effects on peat carbon cycling in a boreal rich fen. *Biogeochemistry,* 144**,** 305-327.

RYDIN, H. & JEGLUM, J. K. 2013. *The Biology of Peatlands*, Oxford University Press.

RYDIN, H., JEGLUM, J. K., RYDIN, H. & JEGLUM, J. K. 2006. Peatland patterns and landforms. *The Biology of Peatlands*. Oxford University Press.
SCHAEPMAN-STRUB, G., LIMPENS, J., MENKEN, M., BARTHOLOMEUS, H. M. & SCHAEPMAN, M. E. 2009. Towards spatial assessment of carbon sequestration in peatlands: spectroscopy based estimation of fractional cover of three plant functional types. *Biogeosciences,* 6**,** 275-284.
SCHWEIGER, A. K., SCHUTZ, M., RISCH, A. C., KNEUBUHLER, M., HALLER, R. & SCHAEPMAN, M. E. 2017. How to predict plant functional types using imaging spectroscopy: linking vegetation community traits, plant functional types and spectral response. *Methods in Ecology and Evolution,* 8**,** 86-95.
SEGAL, M. & XIAO, Y. Y. 2011. Multivariate random forests. *Wiley Interdisciplinary Reviews-Data Mining and Knowledge Discovery,* 1**,** 80-87.
STEENVOORDEN, J., BARTHOLOMEUS, H. & LIMPENS, J. 2023. Less is more: Optimizing vegetation mapping in peatlands using unmanned aerial vehicles (UAVs). *International Journal of Applied Earth Observation and Geoinformation,* 117.
SU, T. F. & ZHANG, S. W. 2017. Local and global evaluation for remote sensing image segmentation. *Isprs Journal of Photogrammetry and Remote Sensing,* 130**,** 256-276.
SUÁREZ, F., SARABIA, A., SANZANA, P., LATORRE, C. & MUÑOZ, J. F. 2024. The Quebrada Negra wetland study: An approach to understand plant diversity, hydrology, and hydrogeology of high-Andean wetlands. *Wiley Interdisciplinary Reviews-Water,* 11.
SZPORAK-WASILEWSKA, S., PIÓRKOWSKI, H., CIEZKOWSKI, W., JARZOMBKOWSKI, F., SLAWIK, L. & KOPEC, D. 2021. Mapping Alkaline Fens, Transition Mires and Quaking Bogs Using Airborne Hyperspectral and Laser Scanning Data. *Remote Sensing,* 13.
TANNEBERGER, F., MOEN, A., BARTHELMES, A., LEWIS, E., MILES, L., SIRIN, A., TEGETMEYER, C. & JOOSTEN, H. 2021. Mires in Europe-Regional Diversity, Condition and Protection. *Diversity-Basel,* 13.
TIAN, F., CAI, Z. Z., JIN, H. X., HUFKENS, K., SCHEIFINGER, H., TAGESSON, T., SMETS, B., VAN HOOLST, R., BONTE, K., IVITS, E., TONG, X. Y., ARDO, J. & EKLUNDH, L. 2021. Calibrating vegetation phenology from Sentinel-2 using eddy covariance, PhenoCam, and PEP725 networks across Europe. *Remote Sensing of Environment,* 260.
TURETSKY, M. R., BOND-LAMBERTY, B., EUSKIRCHEN, E., TALBOT, J., FROLKING, S., MCGUIRE, A. D. & TUITTILA, E. S. 2012. The resilience and functional role of moss in boreal and arctic ecosystems. *New Phytologist,* 196**,** 49-67.
TURETSKY, M. R., KOTOWSKA, A., BUBIER, J., DISE, N. B., CRILL, P., HORNIBROOK, E. R. C., MINKKINEN, K., MOORE, T. R., MYERS-SMITH, I. H., NYKÄNEN, H., OLEFELDT, D., RINNE, J., SAARNIO, S., SHURPALI, N., TUITTILA, E. S., WADDINGTON, J. M., WHITE, J. R., WICKLAND, K. P. & WILMKING, M. 2014. A synthesis of methane emissions from 71 northern, temperate, and subtropical wetlands. *Global Change Biology,* 20**,** 2183-2197.
TURUNEN, J. & VALPOLA, S. 2020. The influence of anthropogenic land use on Finnish peatland area and carbon stores 1950-2015. *Mires and Peat,* 26.
VERWIJST, T. & TELENIUS, B. 1999. Biomass estimation procedures in short rotation forestry. *Forest Ecology and Management,* 121**,** 137-146.
VRIELING, A., MERONI, M., DARVISHZADEH, R., SKIDMORE, A. K., WANG, T. J., ZURITA-MILLA, R., OOSTERBEEK, K., O'CONNOR, B. & PAGANINI, M.

2018. Vegetation phenology from Sentinel-2 and field cameras for a Dutch barrier island. *Remote Sensing of Environment,* 215**,** 517-529.
WANG, J., XIAO, X. M., BAJGAIN, R., STARKS, P., STEINER, J., DOUGHTY, R. B. & CHANG, Q. 2019. Estimating leaf area index and aboveground biomass of grazing pastures using Sentinel-1, Sentinel-2 and Landsat images. *Isprs Journal of Photogrammetry and Remote Sensing,* 154**,** 189-201.
WANG, Q., PUTRI, N. A., GAN, Y. & SONG, G. M. 2022. Combining both spectral and textural indices for alleviating saturation problem in forest LAI estimation using Sentinel-2 data. *Geocarto International*.
WITHARANA, C. & CIVCO, D. L. 2014. Optimizing multi-resolution segmentation scale using empirical methods: Exploring the sensitivity of the supervised discrepancy measure Euclidean distance 2 (ED2). *Isprs Journal of Photogrammetry and Remote Sensing,* 87**,** 108-121.
YU, Z. C. 2012. Northern peatland carbon stocks and dynamics: a review. *Biogeosciences,* 9**,** 4071-4085.
ZHAO, J. J., ZHANG, H. Y., ZHANG, Z. X., GUO, X. Y., LI, X. D. & CHEN, C. 2015. Spatial and Temporal Changes in Vegetation Phenology at Middle and High Latitudes of the Northern Hemisphere over the Past Three Decades. *Remote Sensing,* 7**,** 10973-10995.
ZHOU, R., YANG, C., LI, E. H., CAI, X. B., YANG, J. & XIA, Y. 2021. Object-Based Wetland Vegetation Classification Using Multi-Feature Selection of Unoccupied Aerial Vehicle RGB Imagery. *Remote Sensing,* 13.